

STUDIES OF A FLAT FLAME UNDER IMPRESSED
ELECTRIC AND MAGNETIC FIELDS

Thesis for the Degree of Ph. D.
MICHIGAN STATE UNIVERSITY
Robert Jennings Heinsohn
1963



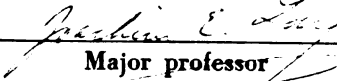
This is to certify that the
thesis entitled
STUDIES OF A FLAT FLAME
UNDER IMPRESSED ELECTRIC AND
MAGNETIC FIELDS

presented by

Robert Jennings Heinsohn

has been accepted towards fulfillment
of the requirements for

Ph. D. degree in Mechanical
Engineering


Major professor

Date May 16, 1963

ABSTRACT

STUDIES OF A FLAT FLAME UNDER IMPRESSED ELECTRIC AND MAGNETIC FIELDS

by
Robert Jennings Heinsohn

A flame contains positive and negative ions which are essential to the kinetics of combustion. By impressing electric and magnetic fields on a flame, it is possible to influence the extinction limits and burning velocity.

The objectives of this research are to devise methods for solving the equations of combustion, and to experimentally study the burning velocity and lean extinction limits of a flat flame under the influence of a perpendicular electric field.

Enlarging upon a method developed by Klein, a method of successive approximations is developed whereby the burning velocity, composition and temperature profiles can be found. The method accommodates an n-species gas and requires only that the species Lewis numbers be near unity, and electromagnetic fields to be constant.

By considering the flame-field interaction to be of mechanical origin describable by a phenomenon known as the Chattock electric wind, it is possible to express the burning velocity as a function of the current through the flame, the positive ion mobility and the usual combustion variables.

The experimental results show that electric fields of either polarity make it possible to support flat flames (seeded with aqueous

KOH mist) at lean fuel-air ratios where extinction would occur if no field were present. Experimental measurements of flame speed agree favorably with approximate theory and show that an electric field parallel to the flow direction increases the flame speed, while a field in the opposite direction reduces the flame speed.

STUDIES OF A FLAT FLAME
UNDER IMPRESSED ELECTRIC AND
MAGNETIC FIELDS

By

Robert Jennings Heinsohn

A THESIS

Submitted to
Michigan State University
in partial fulfillment of the requirements
for the degree of

DOCTOR OF PHILOSOPHY

Department of Mechanical Engineering

1963

To Beth, Janet and Anne, who give purpose to this effort.

ACKNOWLEDGEMENTS

I particularly wish to express my gratitude to my major professor, Dr. Joachim E. Lay, who as teacher, friend and colleague has been a constant source of inspiration and encouragement.

I wish to acknowledge with appreciation the support of my guidance committee, Dr. Carl M. Cooper, Dr. James L. Dye, Dr. Douglas W. Hall, Dr. Roland T. Hinkle and Dr. Joseph A. Strelzoff. The helpful suggestions and enlightening discussions with this committee have been invaluable to me.

I am grateful to Dr. William G. Agnew, of the General Motors Research Laboratories for his assistance in preparing the flow matrix and his constructive suggestions on experimentation.

I wish to acknowledge the Department of Mechanical Engineering for its financial support of this project.

In particular, I am grateful for the friendship of my stalwart office mates Pandeli Durbetaki and Hinrich Martens, and for the opportunity to share with them the exasperation and exhilaration of research.

TABLE OF CONTENTS

Nomenclature	ix
1.	INTRODUCTION AND STATEMENT OF THE PROBLEM	1
2.	BACKGROUND	2
2.1	Historical Review	2
2.2	General Considerations on the Mechanism of Ion Formation	6
3.	GENERAL EQUATIONS OF COMBUSTION IN THE PRESENCE OF AN ELECTRIC AND MAGNETIC FIELD	9
4.	ONE-DIMENSIONAL FLAME	14
4.1	Ion Mobility	16
4.2	Assumptions	17
4.3	Electromagnetic Field Equations	18
4.4	Boundary Conditions	19
4.5	Conservation Equations	21
5.	REDUCED EQUATIONS OF COMBUSTION	25
6.	PROGRAM FOR THE SOLUTION OF THE REDUCED EQUATIONS OF COMBUSTION.	31
6.1	Method of Successive Approximations	31
6.2	Discussion.	38
7.	AN APPROXIMATE THEORY - CHATTOCK ELECTRIC FIELD	43
8.	EXPERIMENTAL EQUIPMENT AND TECHNIQUE	55
8.1	Burner.	55
8.2	Electrostatic Field	55
8.3	Photography	59
8.4	Experimental Technique	59
9.	EXPERIMENTAL RESULTS	61
9.1	Bunsen Burner Flames	61
9.2	Flat Flames Without Seeding	62
9.3	Seeded Flat Flames	65

9.4	Seeded Flat Flames with Positive Electric Fields	69
9.5	Seeded Flat Flames with Negative Electric Fields	77
9.6	Effect of Electric Field on Flame Speed . .	84
	9.6.1 Positive Electric Fields	85
	9.6.2 Negative Electric Fields.	87
10.	CONCLUSIONS	91
	BIBLIOGRAPHY	93
	APPENDICES	101

LIST OF FIGURES

4-1	One dimensional flame	14
7-1	Normal flame in a one-dimensional flow - Positive electric field	44
7-2	Normal flame in a one-dimensional flow - Positive electric field	47
7-3	Effect of electric field intensity upon flame speed	51
7-4	Normal flame in a one-dimensional flow	52
7-5	Positive-ion concentrations in a flat flame	53
8-1	Schematic diagram of burner and atomizer	56
8-2	Schematic drawing of experimental apparatus	57
8-3	Photograph - experimental apparatus	58
8-4	Schematic drawing of the electrical circuit	59
9-1	Distortion of a lean bunsen flame by an electric field	61
9-2	Typical unseeded lean flat-flame without electric field	62
9-3	Current vs applied voltage at constant fuel-air ratio for unseeded flames	64
9-4	Extinction limits of seeded flat flames	67
9-5	Seeded flat flames with positive electric field	71
9-6	Current and voltage vs air flow at extinction, positive electric field, gas flow = .957 li/min	72
9-7	Current and voltage vs air flow at extinction, positive electric field, gas flow = 1.061 li/min	73
9-8	Current and voltage vs air flow at extinction, positive electric field, gas flow = 1.253 li/min	74
9-9	Effect of voltage on the extinction limits of a seeded flat flame, positive electric field	75

9-10	Effect of current on the extinction limits of a seeded flat flame, positive electric field	76
9-11	Seeded flat flames with negative electric field	79
9-12	Effect of a negative field upon the lean extinction limits - current and voltage vs air flow at constant fuel flow	80
9-13	Effect of voltage on the lean extinction limits, negative electric field	81
9-14	Distribution of radicals in a flame subjected to an electric field	83
9-15	Effect of quenching upon flame speed	86
9-16	Flame speed vs current at constant fuel-air ratio and duct velocity - positive electric field	88
9-17	Flame speed vs current at constant fuel-air ratio and duct velocity - negative electric field	90

LIST OF APPENDICES

A -	Equipment	101
B -	Data - Extinction Limits of Seeded Flat Flames	102
C -	Data - Effect of Electric Field Upon Flame Speed	103

NOMENCLATURE

$c_r = \frac{\rho_r}{m_r}$	-	molar concentration (g-moles/cc)
ρ_r	-	mass density (gm/cc)
m_r	-	molecular weight
$c = \sum c_r$	-	molar density of the solution (g-moles/cc)
$x_r = \frac{c_r}{c}$	-	mole fraction
σ_r	-	mass source (g-moles/cc sec)
u_r^i	-	the macroscopic velocity of the r-species (cm/sec)
u^i	-	single-fluid velocity (cm/sec)
t	-	time sec
x^i	-	displacement in the i-direction (cm)
P_r^{ij}	-	stress tensor (dynes/cc)
X_r^i	-	external force per unit volume (dynes/cc)
$(\sigma_r \omega_r)^i$	-	momentum source (due to chemical reaction) per unit vol. (dyne/cc)
v_r^i	-	drift velocity, $v_r^i = u_r^i - u^i$ (cm/sec)
$\bar{e}_r = e_r + \frac{1}{2} \rho_r u_r^2$	-	total energy per unit volume (cal/cc)
e_r	-	internal energy per unit volume (cal/cc)
Q_r^i	-	heat flux (cal/cm ² sec)
\mathcal{E}_r	-	energy source per unit volume (cal/cc sec)
$\mathcal{C}_r = u_r^j X_r^j$	+	viscous heating + joulean heating
T	-	absolute temperature (K)
D_{rs}	-	multicomponent diffusion coefficient (cm ² /sec)
\tilde{G}_s	-	partial molar Gibbs free energy (cal/cc)
\tilde{V}_s	-	partial molar volume (cc g-mole)

D_r^T	-	multicomponent thermal diffusion coefficient (gm/cm sec)
q_r	-	charge density (coul/cc)
γ_r	-	charge to mass ratio (coul/gm)
J^i	-	current density (coul/cm ² sec)
\vec{D}	-	displacement vector (newton/coul)
\vec{E}, \vec{e}	-	electric field intensity (newton/coul, or volt/meter)
\vec{B}, \vec{b}	-	magnetic induction (weber/m ²)
\vec{H}	-	magnetic field intensity (amp/meter)
ϵ_0	-	electric permittivity
μ_0	-	magnetic permeability (K gm-m/coul ²)
N_A	-	Avagadro's number (particles per g-mole)
H_r	-	enthalpy of pure species r, $H_r = m_r h_r$ (cal/g-mole)
h_r	-	enthalpy of pure species r, $h_r = (e/\rho)_r + (p/\rho)_r$ (cal/gm)
λ	-	thermal conductivity (cal/degree sec cm)
V	-	electric potential (volts)
n_r	-	number of particles per cc ($n_r = n_+$ or n_-)
k_j	-	reaction rate constant (with appropriate units)
K_r	-	ion mobility (signed) (cm/sec per volt/cm)
d	-	electrode separation (cm)
E_r^*	-	Activation energy (cal/g-mole)
ρ	-	single-fluid mass density, $= \sum_{r=1}^n \rho_r$ (gm/cc)
q	-	single-fluid charge density, $q = \sum_{r=1}^n q_r$ (coul/cc)

- \bar{m} - average molecular weight, $\bar{m} = \frac{\rho}{c} = \sum_{r=1}^n x_r m_r$
 (gm/cc)
- e - single-fluid internal energy, $e = \sum_{r=1}^n (e_r + \rho_r v_r^2 / 2)$
 (cal/cc)
- \bar{e} - total single-fluid internal energy, $\bar{e} = \sum_{r=1}^n e_r = e + \rho u^2 / 2$
 (cal/cc)
- X^i - single-fluid external force, $X^i = \sum_{r=1}^n X_r^i$, (dynes/cc)
- \mathcal{E} - single-fluid external force, $\mathcal{E} = \sum_{r=1}^n \mathcal{E}_r$, (cal/cc sec)
- P^{ij} - single-fluid stress tensor, $P^{ij} = \sum_{r=1}^n (P_r^{ij} + \rho_r v_r^i v_r^j)$
 (dynes/cm²)
- Q^i - single-fluid energy flux, $Q^i = \sum_{r=1}^n (Q_r^i + u_r^j P_r^{ij} + \bar{e}_r u_r^i) -$
 $(\bar{e} u^i + u^j P^{ij})$ cal/cm² sec
- G_r^i - fraction of the mass rate of flow, $G_r^i = \frac{\rho_r u_r^i}{\rho u^i}$
- M^i - momentum of the single-fluid, $M^i = \rho u^i$
- R - universal gas constant (atm cc/g-mole K)
- \mathcal{R} - gas constant, $\mathcal{R} = R / \bar{m}$ (atm cc/gm K)
- C_p, C_v - single-fluid specific heats (cal/g-mole K)
- c_{p_r}, c_{v_r} - specific heat of pure species r (cal/gm K)
- c^* - single-fluid speed of sound (cm/sec)

1. INTRODUCTION AND STATEMENT OF THE PROBLEM

A flame contains positive and negative ions which are formed as intermediate species in the complex chemical kinetics of combustion. In addition to their role in the chemical kinetics, these ions also enter into the momentum exchanges which accompany combustion. Electric and magnetic fields exert forces on moving charged particles. It is therefore reasonable to suspect that impressing an electric and/or magnetic field on a flame will alter the outward characteristics of the flame by influencing both the ion-molecule momentum exchanges and the overall characteristics of the chemical reaction.

This research is concerned with the outward characteristics of a flame under impressed electromagnetic fields, with particular interest in the flame speed and the lean extinction limits. The specific objectives of this research are threefold:

- (1) to devise a method to solve the exact equations of combustion for a steady-state, plane combustion wave under the influence of electric and magnetic fields;
- (2) to devise an approximate theory which predicts the burning velocity of a flame under the influence of an electric and magnetic field;
- (3) to experimentally study the burning velocity and lean extinction limits of a flat flame under the influence of a perpendicular electric field.

2. BACKGROUND

2.1 Historical Review

In 1801, Volta showed that the leaves of a gold-leaf electroscope diverged when burning charcoal was brought in contact with the knob⁽¹⁸⁾. The research which followed was chiefly concerned with measuring the electrical conductivity of flames. From these studies, it was found that the conduction property could be lessened or removed by passing the combustion gases through an electric field of appropriate strength. Complete accounts of these early discoveries are to be found in Widemann's "Elektricität"⁽²⁰⁾, and in a paper by de Hemptinne⁽²¹⁾.

The development of the ionic theory of the electrical properties of gases by Sir J. J. Thomson in the late 19th century led to numerous investigations, which quite naturally included an examination of flames. Two splendid accounts of the research from 1900 to 1930 are in works by J. J. Thomson⁽¹⁸⁾ and H. A. Wilson^(19, 67).

In the period from approximately 1920 to 1930, considerable interest was shown toward influencing or possibly arresting^(23, 24) the propagation of a flame by an electric field. The influence of an electric field is dramatic, and in all cases directs a flame toward the negatively charged electrode, i. e. the direction of positive ion flow. In countless experiments involving axial electric fields^(15, 24, 25, 27, 28) it was qualitatively found that flame speed is either increased or decreased depending on the direction of the field. In experiments

involving transverse fields^(15, 23, 24, 34, 53, 55), a flame was always deflected toward the negative electrode. It was thought that positive ions, of molecular size, were able on collision with ordinary molecules to transfer momentum, and so the whole body of the gas would be driven in the same direction as the positive ions. The much lighter electrons and the relatively few negative ions were not, however, able to have an appreciable counterbalancing effect in the opposite direction. This well-known effect was referred to as the "Chattock electric wind."

Reports of the complete extinction of the flame by an electric field were recorded by Malinowski^(24, 25) (between 1930 and 1936), but whether such extinction was attributable to the field or to the excessive cooling between the enlarged flame and cool surface was never clearly determined. During this same period, attention was directed to the question of whether ionization in the flame was of chemical or thermal origin⁽³⁰⁾. Even though the transport and production mechanism of combustion ions is not even now fully known, Lewis⁽¹⁵⁾ contended in 1931 that the electric field had no effect on either the character or speed of the chemical reaction. From spectroscopic measurements of propane diffusion flames and transverse electric fields, Nakamura⁽⁵⁷⁾ showed that neither the number nor extent of excitation of the radicals in a flame were affected; only the distribution of radicals seemed to be displaced by an externally applied electric field.

In the last ten years, a concentrated effort has been made to determine the origin, identity and concentration of combustion ions.^(26, 31, 41, 42, 43, 44, 57, 58, 59, 60, 61, 62, 65)

A comprehensive review of this work and more recent findings can be found from the leading investigators in this field Sudgen⁽⁶⁹⁾, Van Tigglen⁽⁶⁴⁾, and Calcote^(60,68).

Earlier thoughts⁽³⁰⁾ that combustion ions resulted from thermal ionization via the Saha equation,⁽⁴⁹⁾

$$\log_{10} K_{eq} = -\frac{5050V}{T} + \frac{3}{2} \log_{10} T + 15.38 + \log_{10} \frac{g_{M^+} g_{e^-}}{g_M} \quad (2-1) \quad *$$

where



$$K_{eq} = \frac{[M^+][e^-]}{[M]} \quad (2-3)$$

have been dispelled since the ionization potentials (V) of all known combustion species or possible contaminants were too high to produce the large ion densities observed by experiment,⁽⁴³⁾ The Saha equation predicted ion densities many orders of magnitude less than those found experimentally. The responsible mechanism is now thought to be "chemi-ionization,"^(60,61,62,68,69) ionization resulting directly from a chemical reaction having the form,



While the literature is rich with research concerning electric fields, little record can be found concerning an interest in, or success with magnetic fields. In 1931, Dixon, Campbell and Slater⁽³³⁾ photographically studied the effect of a transverse magnetic field of 10^4

* g_{M^+} , g_{e^-} , g_M are statistical weights, for an alkali metal this term is zero.

gauss on the detonation wave in mixtures with oxygen of hydrogen, acetylene, cyanogen, carbon monoxide and carbon disulphide. There was no visible influence on the speed or form of any of the detonation waves nor, in experiments with acetylene and oxygen, could any alternation in the initiatory phases of the explosion flames be detected. On the other hand, J. S. Watt⁽⁶⁷⁾ reported that the upward motion of a flame was stopped with a magnetic field in one direction and greatly accelerated with it in the other direction, if the flame was seeded with potassium and a current of 4×10^{-2} amps was used.

The Hall effect in flames has been experimentally measured by Marx⁽³²⁾ and Wilson^(19, 67). Measurements by Wilson⁽⁶⁷⁾ and Thomson⁽¹⁹⁾ found an appreciable difference in flame conductivity due to the Hall currents produced by a magnetic field. In a recent study, Beck^(8, 37) analytically showed that if the gases of a flame had infinite conductivity a large steady magnetic field markedly increased the flame speed.

There has always been an interest in applying electromagnetic fields to combustion processes. The original suggestion of magneto-hydrodynamic power generation is credited to Faraday⁽²²⁾ who proposed the use of a fluid rather than a solid conductor in a generator. Although Faraday did not propose the use of an ionized gas, there is presently considerable engineering interest^(63, 84, 85) in this country and Europe in flames seeded with alkali metals and their use in power generation. In addition to power generation, engineers have continually

explored the use of electromagnetic fields for the improvement of mixing processes of combustion⁽³⁶⁾, heat transfer⁽⁵³⁾, carbon deposition^(53,80), anti-knock mechanism for internal combustion engines⁽²⁹⁾.

The literature records many experimental investigations concerning fields, but relatively few solutions of the formidable equations describing combustion phenomena and electromagnetic fields. Studies based upon Thompson's ionic theory of gases^(11,12,18,19,36,53,55,67), lend themselves to simple analysis but suffer because diffusion and chemistry are overly simplified. On the other hand, the more exact solutions of Spalding,^(70,71,72,73) Hirschfelder,^(2,9,39,40,51,79) Penner and von Karman,^(17,38,78,89) Klein,^(35,74,75) and others^(70,92) exclude external forces arising from applied electric and magnetic fields and are extremely difficult to solve.

2.2 General Considerations on the Mechanism of Ion Formation

One of the most active phases in the whole subject of combustion is the investigation of flame ionization. Without comment, a brief resume of the generally accepted theory^(60,61,68,69,94) of ion formation will be presented. Many reaction paths might appear feasible, but the acceptance of two simple rules reduces this to a limited number. These rules require that the ion-producing reaction should be exothermic or mildly endothermic, and that the reactants should be simple species which are known to be present in hydrocarbon flames.

The most abundant positive ion found in hydrocarbon flames is H_3O^+ ^(59,66,68,69) and the predominant negative ion is the free

electron. Different hydrocarbon-air (or oxygen) flames have different ion profiles but all flames produce a total ion concentration of the order of 10^{10} ions per cc. Inside the visible portion of the flame, the formation and disappearance of H_3O^+ is thought to be governed by,



Thermodynamic estimates by Sudgen⁽⁶⁹⁾ are,

$$k_3 = 2.2 \pm 1.0 \times 10^{-7} \text{ cm}^3 \text{ sec}^{-1} \quad (2-6)$$

$$\Delta h = - 145 \text{ Kcal} \quad (2-7)$$

Formation of H_3O^+ is thought^(68,69) to be a proton transfer from a carbon-bearing precursor, CHO^+ , by the reaction



with thermodynamic estimates,⁽⁶⁹⁾

$$k_2 = 10^{-8} \text{ cm}^3 \text{ sec}^{-1} \quad (2-9)$$

$$\Delta h = - 34 \text{ Kcal} \quad (2-10)$$

In accord with earlier rules of thermoneutrality, the reaction favoring the formation of the precursor is,



The origin of H, O, CH is not as clearly known or agreed upon, but all are simple species which have been observed as reaction zone constituents. Thermodynamic data for the last reaction are thought⁽⁶⁹⁾ to be,

$$k_1 = 3 \times 10^{-12} \text{ cm}^3 \text{ sec}^{-1} \quad (2-12)$$

$$\Delta h \cong 0 \text{ Kcal}$$

(2-13)

The chemical kinetics describing combustion in the quenching zone (i.e. from cold boundary to reaction zone) and downstream of the reaction zone (i.e. from reaction zone to hot boundary), are not generally agreed upon.

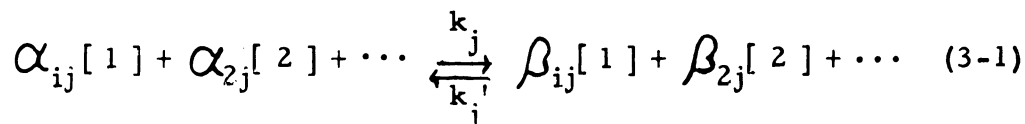
3. GENERAL EQUATIONS OF COMBUSTION IN THE PRESENCE OF ELECTRIC AND MAGNETIC FIELDS

An inescapable preliminary to the calculation of flame speed, temperature and species profiles is the evaluation, from knowledge or assumptions about the reaction kinetics of the flame, of the dependence of volumetric reaction rate on temperature and gas composition for the entire region between hot and cold boundary.

In quantitative discussions of combustion and particularly in laminar flame propagation it is customary to introduce the fundamental postulate that chemical reaction rates applicable for the isothermal conditions corresponding to temperatures, pressures and concentrations may be used in flow problems with temperature and concentration gradients.

(3, 9, 17, 78, 89) This assumption meets with fundamental difficulties only in those cases in which the gradients are so large that the concepts of local temperature, pressure and concentration lose their significance. This situation does not occur for the flames under consideration and the rates of formation σ_r , will be taken to be the same as those applying in a static system under the same conditions of temperature, pressure and composition.

For a general system consisting of n chemical species, it is assumed that the overall reaction proceeds according to a set of, p , chemical reactions which have the stoichiometrical form:



where α, β and [1], [2], etc. refer respectively to the number of moles and the species in the stoichometric equation. The subscripts $ij, 2j$, etc. denote the stoichometric coefficients of the 1st, 2nd, etc. species in the j th chemical reaction. If k_j and k_j' are the specific reaction-rate constants for the forward and reverse reactions respectively, the net rate, r_j , of the j th reaction is according to the law of Mass Action:

$$r_j = k_j(T) c^{\bar{\alpha}_j} x_1^{\alpha_{1j}} x_2^{\alpha_{2j}} \dots - k_j'(T) c^{\bar{\beta}_j} x_1^{\beta_{1j}} x_2^{\beta_{2j}} \dots \quad (3-2)$$

$$\bar{\alpha}_j \equiv \sum_{r=1}^n \alpha_{rj} \quad \bar{\beta}_j \equiv \sum_{r=1}^n \beta_{rj}$$

Thus σ_r , the number of molecules of the r -th species that are produced by chemical action per second per cc is given by:

$$\sigma_r = \sum_{j=1}^P (\beta_{rj} - \alpha_{rj}) r_j \quad , \quad r = 1, 2, 3, \dots, n \quad (3-3)$$

In static systems it is convenient, and in most cases sufficiently accurate, to express the specific rate constants by the Arrhenius expression,

$$k_j(T) = A_j \exp(-E_j^*/RT) \quad (3-4)$$

where A_j and E_j^* are the sterric factor and activation energy respectively.

The chemical reactions take place in a gaseous environment which possesses certain gross or "single-fluid" properties. The single fluid

moves with a velocity u^i and each species (r) moves with a velocity v_r^i relative to the single-fluid. The superscript i, j or k denote the components of a Cartesian tensor.

The conservation equations for each species, r, of a homogeneous n-component chemically reacting flow system are as follows: (2, 3, 4, 6, 7, 9, 17, 89)

continuity

$$\frac{\partial \rho_r}{\partial t} + \frac{\partial}{\partial x^j} (\rho_r u_r^j) = m_r \sigma_r, \quad (3-5)$$

momentum

$$\frac{\partial}{\partial t} (\rho_r u_r^i) + \frac{\partial}{\partial x^j} (\rho_r u_r^i u_r^j + P_r^{ij}) = X_r^i + \sigma_r \omega_r^i \quad (3-6)$$

energy

$$\frac{\partial}{\partial t} \bar{e}_r + \frac{\partial}{\partial x^j} (\bar{e}_r u_r^j + u_r^i P_r^{ij} + Q_r^j) = \mathcal{E}_r \quad (3-7)$$

diffusion

$$\begin{aligned} (\rho_r v_r^i)^i = & \frac{c^2}{\rho RT} \sum_{s=1}^n m_r m_s D_{rs} \left[x_s \sum_{\substack{t=1 \\ t \neq s}}^n \left(\frac{\partial \tilde{G}_s}{\partial x_t} \right)_{T,p,x_q} \left(\frac{\partial x_t}{\partial x^i} \right) \right] \\ & + \frac{c^2}{\rho RT} \sum_{s=1}^n m_r m_s D_{rs} \left[x_s m_s \left(\frac{\tilde{v}_s}{m_s} - \frac{1}{\rho} \right) \frac{\partial p}{\partial x^i} \right] \\ & - \frac{c^2}{\rho RT} \sum_{s=1}^n m_r m_s D_{rs} \left[x_s m_s \left(\frac{X_r^i}{\rho_r} - \sum_{t=1}^n \frac{X_t^i}{\rho} \right) \right] \\ & - D_r \frac{T}{\rho} \frac{\partial \ln T}{\partial x^i} \end{aligned} \quad (3-8)$$

Subject to the definitions of the gross properties of the single-fluid the conservation equations are:

continuity

$$\frac{\partial \rho}{\partial t} + \frac{\partial}{\partial x^j} (\rho u^j) = 0 \quad (3-9)$$

momentum

$$\frac{\partial}{\partial t} (\rho u^i) + \frac{\partial}{\partial x^j} (\rho u^i u^j + P^{ij}) = X^i \quad (3-10)$$

energy

$$\frac{\partial \bar{e}}{\partial t} + \frac{\partial}{\partial x^j} (\bar{e} u^j + u^i P^{ij} + Q^j) = \mathcal{E} \quad (3-11)$$

In addition to the conservation equations, it is also necessary to introduce an equation of state. In this study, the gases will be considered to be ideal.

$$p_r = c_r RT \quad (3-12)$$

$$p = cRT \quad (3-13)$$

It is convenient to define a term G_r^i as the fraction of the mass rate of flow of the r-th species.

$$G_r^i = \frac{\rho_r u_r^i}{M^i} = \frac{c m_r x_r u_r^i}{M^i} \quad (3-14)$$

where,

$$M^i = \rho u^i \quad (3-15)$$

The equations describing the electric and magnetic fields are Maxwell equations. Relative to the stationary reference system, Maxwell's equations in vector form are,

$$\operatorname{div} \vec{D} = q \quad (3-16)$$

$$\operatorname{div} \vec{B} = 0 \quad (3-17)$$

$$\operatorname{curl} \vec{E} = - \frac{\partial \vec{B}}{\partial t} \quad (3-18)$$

$$\operatorname{curl} \vec{H} = \vec{J} + \frac{\partial \vec{D}}{\partial t} \quad (3-19)$$

The constituent field relationships are

$$\vec{D} = \epsilon \vec{E} \quad (3-20)$$

$$\vec{B} = \mu \vec{H} \quad (3-21)$$

4. ONE-DIMENSIONAL FLAME

A sketch of an idealized one-dimensional flame is as follows,

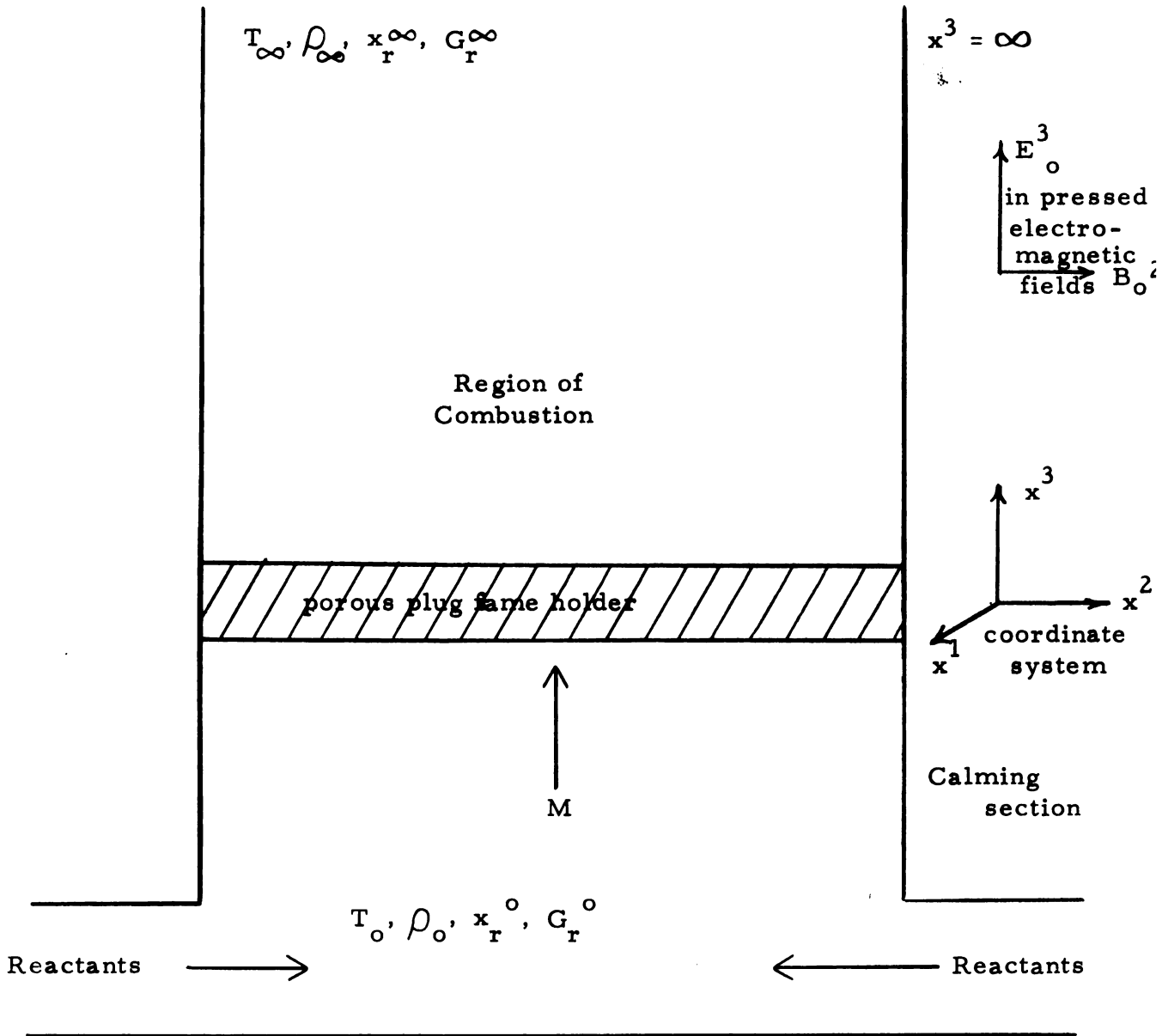


Fig. 4-1

One dimensional flame

where E_o^3 , B_o^2 are the flux densities of the externally applied electric and magnetic fields. Gases flow is in the x^3 direction and combustion is assumed to take place in the $x^1 x^2$ plane. Fluid properties are assumed to be uniform in planes parallel to the $x^1 x^2$ plane, and thus are spatial variations of x^3 alone.

While fluid properties display only x^3 variations, the same is not necessarily true of electromagnetic properties. If there exists an electric current density J^3 in a magnetic field B^2 , a transverse electric field, E^1 and transverse current density J^1 are induced. The general explanation of this effect, which is analogous to the "Hall effect" in metals, is easy; the calculation of the magnitude is difficult. A rigorous treatment necessitates a two-dimensional approach to the problem. As the Hall currents are small and as a one dimensional

problem is more easily solved an approximate method employing the transport property "mobility" will be used to evaluate the transverse current (J^1) and the related drift velocities (v_+^1, v_-^1).

4.1 Ion Mobility

While the force Ee , acting upon an ion of charge e in an electrostatic field E , induces a steady acceleration in a vacuum, an ionic velocity, constant for each given value of E , is observed at appreciable pressures. This implies that owing to ion-molecule collisions, a state of equilibrium is attained in which the additional energy gained by the ion in traveling a mean free path is on the average given up in the collision which terminates it. The effective mean free path is not necessarily that calculated on simple kinetic theory. Thus in the case of an electron starting from rest, energy transfer to molecules is very small during initial elastic collisions and its additional energy increases to a high value before equilibrium is obtained. Since ions do not continue to accelerate, however, the largest part of the potential energy due to their initial position in the field is imparted to the gas. The ion itself retains only the additional kinetic energy due to its drift velocity which is a negligible fraction of the total energy as long as the effective mean free path is negligible in comparison with distances traveled.

The drift velocity of ions is proportional to the field strength providing the ions are in thermal equilibrium with the gas molecules,

$$v_+^i = K_+ E^i \quad (4-1)$$

$$v_-^i = K_- E^i \quad (4-2)$$

This relationship is valid for field strengths from zero to approximately 16,000 volts/cm. (at 1 atm). The experimental field strengths in this study are well within these limits. Above, 16,000 volts/cm, the ions gain energy from the field in a mean free path, comparable in amount to the thermal energy of the gas molecules, thermal equilibrium no longer exists, and the proportionality between drift velocity and the first power of field strength is then not applicable.

In the case of electrons, fields much smaller than 16,000 volts/cm (at 1 atm), suffice for electrons to gain energy for the field between collisions, in excess of that which they would have if in thermal equilibrium with the gas. The situation is further complicated by inelastic collisions between electrons and molecules, in which case the electronic mobility is not independent of the field strength. However, the drift velocity of electrons is of the order of 10^3 times that of ions in similar fields and the mobilities are in the same ratio. For simplicity, it has been assumed, therefore, that the drift velocity of electrons is proportional to the field strength. The results of ion mobility measurements given by Wilson⁽⁵⁶⁾ and Kinbara and Ikegami⁽⁵⁸⁾ suggest values of $1 \text{ cm}^2 \text{ volt}^{-1} \text{ sec}^{-1}$ for positive and $10^3 \text{ cm}^2 \text{ volt}^{-1} \text{ sec}^{-1}$ for negative ions.

4.2 Assumptions

In addition to the notion of mobility, the following additional assumptions will be made:

- (1) all time derivatives are zero (i.e. steady state)
- (2) gases are ideal and the specific heats are constant, ions

behave as if they were ideal gas components

- (3) flame is infinite in the x^1, x^2 directions such that $u_r^2, =$
 $u^2 = v_r^2 = 0, u^1 = 0$
- (4) $u^3 = u^3(x^3), v_r^3 = v_r^3(x^3), u_r^3 = u_r^3(x^3), T = T(x^3)$
 $p = p(x^3), \rho = \rho(x^3)$
- (5) the region of combustion is adiabatic; and external energy sources and kinetic energies are negligible in comparison to thermal energies
- (6) pressure and thermal diffusion are negligible
- (7) the ideal gas mixture has constant values of $\epsilon = \epsilon_0, \mu = \mu_0$
- (8) the external forces are expressible by the Lorentz equation,

$$\vec{X}_r = q_r [\vec{E} + \vec{u}_r \times \vec{B}]$$

- (9) the gases are inviscid and, the stress tensor and heat flux are

$$P_r^{ij} = \delta^{ij} P_r, \quad \delta^{ij} = \begin{cases} 0 & i \neq j \\ 1 & i = j \end{cases}$$

and

$$Q^i = \lambda \left(\frac{dT}{dx^i} \right)$$

- (10) the external force X^3 in the momentum equation can be neglected

4.3 Electromagnetic Field Equations (14, 76, 77)

Relative to stationary reference system, the force (X_r^3) on a charged particle is,

$$X_r^3 = q_r [E^3 + u_r^1 B^2 - u_r^2 B^1] \quad (4-3)$$

The field components arising from the space charges will be considered perturbations (\vec{b}, \vec{e}) on the uniform applied fields E_o^3, B_o^2 . These perturbations then must satisfy equations (3-16-2i). As the space charge density is small and its spatial derivatives also small, and as the applied fields are sufficiently large, it will be assumed that

$E_o \gg e, B_o \gg b$ and that Maxwell's equations are satisfied by,

$$\vec{E} = E_o^3 = \text{const} \quad (4-4)$$

$$\vec{B} = B_o^2 = \text{const} \quad (4-5)$$

Since the macroscopic flow velocity $u = u^3$, the magnetic field is seen to contribute a force X_r^3 only as a result of a drift velocity v_r^1 . Thus (4-3) becomes

$$X_r^3 = q_r [E_o^3 + v_r^1 B_o^2] \quad (4-6)$$

4.4 Boundary Conditions

The uniform magnetic field (B_o^2) is applied externally by a device which imposes no solid boundaries or length requirements in any direction. The uniform electric field (E_o^3) is produced by applying a potential difference across electrode screens located in $x^1 x^2$ planes.

The electrodes are idealized screens through which the uncharged gas species pass undisturbed, but gather charged species of unlike sign in a sheath adjacent to the electrode. Within the sheath, these charges migrate toward the electrode, are absorbed by the electrode through some complex process and give rise to currents in the microampere range. Thus ion velocities are identically zero at each boundary and the mole fraction for ions of like sign with the electrode are also zero.

At infinity, the hot boundary, complete thermal and chemical equilibria are required in order to permit a true "burned" stationary state. Consequently, all fluid properties have gradients which are zero at infinity. Since drift velocities of uncharged particles are due to concentration gradients, the drift velocity of uncharged species is zero at infinity. The mole fraction x_r at infinity is determined by requiring all production rates σ_r to be zero. Thus, at infinity, the hot boundary conditions are,

$$G_r = \left(\frac{mc}{\rho_\infty} \right) (x_r)_\infty \quad (4-7)$$

$$G_+ = 0 \quad (4-8)$$

$$G_- = 0 \quad (4-9)$$

These equations, as others to follow, contain notational simplifications brought about by the assumption of Section 4.2. They are as follows

$$G_r^3 = G_r^3, \quad M = M^3, \quad E^3 = E_o^3, \quad B^2 = B_o^2$$

At $x^3 = 0$, the cold boundary, the flame holder serves as both a heat sink, electrode and a device to prevent the diffusion of combustion products into the calming section. The flame holder extracts an amount of heat from the flame equal to,

$$Q_o^3 = - \lambda_o \left(\frac{dT}{dx^3} \right)_o \quad (4-10)$$

The heat transfer while small, lends stability to the position of the flame. For simplicity, it will be considered to be zero in this study,

$$\text{viz. } \left(\frac{dT}{dx^3} \right)_0 = 0.$$

The temperature (T_0) and pressure (p_0) are known in the calming section and have the same value at the cold boundary. The values of $(x_r)_0$ will be assumed to be those that exist in the calming section. Thus as pure reactants and no charged species exist in the calming section,

$$G_r = \left(\frac{mc}{\rho_0} \right) (x_r)_0 \quad (4-11)$$

$$G_+ = G_- = 0 \quad (4-12)$$

4.5 Conservation Equations

Subject to the previous assumptions, the conservation equations of Chapter 3 reduce to the following:

- (1) The equation of continuity for the single-fluid:

$$M = \rho u^3 = \text{constant} \quad (4-13)$$

- (2) The equations of conservation of chemical species:

$$M \frac{dG_r}{dx^3} = m_r \sigma_r \quad (4-14)$$

The related normalizing equations are,

$$\sum_{r=1}^n x_r = 1, \quad \sum_{r=1}^n G_r = 1 \quad (4-15)$$

- (3) The equation of conservation of momentum for the single

fluid:

$$(p_0 - p_\infty) + M(u_0^3 - u_\infty^3) + \sum_{r=1}^n [(\rho_r v_r^3 v_r^3)_0 - (\rho_r v_r^3 v_r^3)_\infty] = 0 \quad (4-16)$$

If R is the gas constant, c^* the speed of sound, and c_p and c_v the specific heats of the single fluid,

$$p = \rho RT \quad (4-17)$$

$$c^* = \left(\left(\frac{c_p}{c_v} \right) RT \right)^{1/2} \quad (4-18)$$

then (4-16) can be written as

$$\left[\frac{p_o - p_\infty}{p_o} \right] + \left(\frac{c_p}{c_v} \right) \frac{u_o^3 (u_o^3 - u_\infty^3)}{(c_o^*)^2} + \frac{c_p}{c_v} \sum_{r=1}^n \left[x_{r_o} \left(\frac{v_r^3}{c^*} \right)_o^2 + x_{r_\infty} \left(\frac{v_r^3}{c^*} \right)_\infty^2 \right] = 0 \quad (4-19)$$

Since representative combustion velocities at $x^3 = 0$ are 30 cm/sec, and at $x^3 = \infty$ are 300 cm/sec, with $c_o^* = 30,000$ cm/sec, it may be concluded that the pressure very nearly remains constant throughout the combustion zone. Thus the momentum equation is satisfied by $p = p_o = \text{constant}$. From experiment⁽¹¹⁾, it is known that under an electric field, the pressure drop across a flame is of the order of .06 cm of H_2O , and of this roughly 10% is attributable to the applied electric field. Consequently, even in the presence of electromagnetic fields, the assumptions appear reasonable.

(4) The equation of state:

$$p = cRT \quad (4-20)$$

(5) The equation of conservation of energy for the single fluid:

$$\frac{d}{dx^3} \left[-\frac{\lambda}{M} \frac{dT}{dx^3} + \sum_{r=1}^n G_r h_r \right] = 0 \quad (4-21)$$

If h_r^∞ is the enthalpy at the definite temperature T_∞ then

$$h_r = h_r^\infty - (c_p)_r (T_\infty - T) \quad (4-22)$$

and the integrated form of (4-21) becomes,

$$\frac{\lambda}{M} \frac{dT}{dx^3} = \sum_{r=1}^n G_r h_r^\infty - \left[\sum_{r=1}^n G_r^\infty h_r^\infty + \sum_{r=1}^n G_r (c_p)_r (T_\infty - T) \right] \quad (4-23)$$

It is convenient⁽³⁵⁾ to write the enthalpy terms relative to h_B ,

where B is a particular component of the combustion species r. Let

B be the last or (one of) the main combustion produce (s); more

definitely, the component for which h_r is the least, though, this is

not essential. Thus, (4-23) may be written as

$$\begin{aligned} \frac{\lambda}{M} \frac{dT}{dx^3} = & \sum_{r=1}^n (h_r^\infty - h_B^\infty) G_r \\ & - \left[\sum_{r=1}^n (h_r^\infty - h_B^\infty) G_r^\infty + \sum_{r=1}^n G_r (c_p)_r (T_\infty - T) \right] \end{aligned} \quad (4-24)$$

Define the "single fluid energy flux" Q^* as,

$$Q^* \equiv -\lambda \frac{dT}{dx^3} + \sum_{r=1}^n v_r^3 \rho_r h_r \quad (4-25)$$

This heat flux represents the gain in energy through conduction plus that transported by diffusion. At the hot and cold boundaries where the temperature gradient and drift velocities are zero, the heat flux is zero. Elsewhere the heat flux will not, in general, vanish and it is of interest to consider its functional form.

(6) The equations of diffusion:

Using the Lorentz equation and the notion of mobility to evaluate the transverse drift velocity (v_+^1, v_-^1) , the diffusion equations may be written as

$$\frac{dx_r}{dx^3} = \frac{M}{c} \sum_{r \neq s=1}^m \left(\frac{x_r^m G_r - x_s^m G_s}{D_{rs}^m m_r m_s} \right) +$$

$$\left(\frac{x_r^m}{p} \right) c E_o^3 \left[\gamma_r - \sum_{r \neq s=1}^n x_s \left(\frac{m_s}{m} \right) \gamma_s \right] -$$

$$\left(\frac{x_r^m}{p} \right) \frac{M}{m} (B_o^2)^2 \left[\gamma_r^{K_r(T)} - \sum_{r \neq s=1}^n \left(\frac{m_s}{m} \right) \gamma_s^{K_s(T)} \right] \quad (4-26)$$

5. REDUCED EQUATIONS OF COMBUSTION

A solution of the equations of combustion allows one to find the temperature and species mole fractions as functions of distance (x^3) from hot to cold boundary. In addition, the parameter M divided by the density at the cold boundary is the flame speed.

Solutions to the equations of a one-dimensional flame in which the effects of radiation, thermo-diffusion, viscosity, and variation of pressure are neglected have been made by Hirschfelder^(2, 9, 39, 51), Spalding^(70, 71, 72, 73) and others^(17, 38, 74, 75, 89) and have been widely published throughout the last ten years. While the external forces that would be created by externally impressed electric or magnetic fields have not been considered, the procedures of Hirschfelder and Spalding served as a useful structure from which it seemed possible to obtain solutions to the more general problem. Of particular value to this study were the techniques of Klein^(35, 74, 75), which without too much difficulty were expanded to include electromagnetic effects.

The diffusion equations are seen to be non-linear and along with the different masses and specific heats of the species are chiefly responsible for the complexity of the problem. As suggested by Klein⁽³⁵⁾, it will be convenient to introduce certain constants so that the variables of the problem might be changed and the equations remodeled in a form amenable to computer solution. The following constants will be introduced,

$$E = \sum_{r=1}^n m_r (h_r^\infty - h_B^\infty) x_r^0 \quad (5-1)$$

$$\delta_{sr} = \frac{D_{rs} m c c_p}{\lambda} \quad (5-2)$$

$$b_r = (m c_p) / R \quad (5-3)$$

$$b = \left(\frac{m c_p}{R} \right) = \sum_{r=1}^n b_r x_r^0 \quad (5-4)$$

$$a = 1 - b(\mathcal{T}_\infty - \mathcal{T}_0) \quad (5-5)$$

$$L_r = m_r (h_r^\infty - h_B^\infty) / E \quad (5-6)$$

$$m = \sum_{r=1}^n m_r x_r^0 \quad (5-7)$$

The reduced variables are,

temperature,

$$\mathcal{T} = RT/E; \quad (5-8)$$

distance,

$$\frac{d\zeta}{dx^3} = \frac{M c_p}{\lambda}, \quad \zeta = M \int_0^{x^3} (c_p / \lambda) dx^3 \quad (5-9)$$

and flow,

$$y_r = \left(\frac{m}{m_r} \right) G_r \quad (5-10)$$

such that now,

$$\sum_{r=1}^n \left(\frac{m}{m_r} \right) y_r = 1 \quad (5-11)$$

In the manipulation of equations which follows, it is convenient to invent a dimensionless temperature gradient, g , which relates reduced distance and temperature, viz.,

$$g = \frac{dT}{d\zeta} \quad (5-12)$$

In terms of reduced variables, the conservation equations become:

energy

$$bg = \sum_{r=1}^n L_r y_r - \left[a + \sum_{r=1}^n b_r y_r (\tau_\infty - \tau) \right] \quad (5-13)$$

Defining ϕ as the reduced single fluid energy flux Q^*

$$Q^* = \left(\frac{ME}{m} \right) \phi \quad (5-14)$$

one finds that the single fluid energy flux may be written as

$$\phi = -bg + \sum_{r=1}^n \left[y_r - \left(\frac{m}{M} \right) x_r \right] \left[L_r - b_r (\tau_\infty - \tau) \right] \quad (5-15)$$

Eliminating (bg) from the energy equation, the single fluid energy flux

becomes,

$$\phi = a - \left(\frac{m}{M} \right) \sum_{r=1}^n x_r \left[L_r - b_r (\tau_\infty - \tau) \right] \quad (5-16)$$

species

$$g \left(\frac{dy_r}{d\tau} \right) = b \alpha q \sigma_r \quad (5-17)$$

where,

$$q = \lambda(\tau) / \lambda(\tau_0) \quad (5-18)$$

$$\alpha = \left(\frac{1}{b} \right) \left(\frac{m}{M} \right)^2 \frac{\lambda(\tau)}{R} \quad (5-19)$$

momentum

$$p = p_o = \text{constant} \quad (5-20)$$

diffusion

$$g\left(\frac{dx_r}{d\tau}\right) = \sum_{s \neq r=1}^n \frac{1}{\delta_{sr}} (x_r y_s - x_s y_r) + \Gamma_r^E + \Gamma_r^M \quad (5-21)$$

where

$$\Gamma_r^E = \left[\frac{bcE_o^3 [R\lambda(\tau_o)]^{1/2}}{p c_p} \right] q \alpha^{1/2} x_r \left(\frac{m_r}{m}\right) \left(\gamma_r - \sum_{s \neq r=1}^n x_s \frac{m_s}{m} \gamma_s \right) \quad (5-22)$$

$$\Gamma_r^M = \left[\frac{\lambda(\tau_o) q (B_o^2)^2}{p c_p} \right] x_r \left(\frac{m_r}{m}\right) \left(-\gamma_r K_r(T) + \sum_{s \neq r=1}^n x_s \left(\frac{m_s}{m}\right) \gamma_s K_s(T) \right) \quad (5-23)$$

Solution of the differential equations is made considerably easier if following Klein⁽³⁵⁾, one assumes that the binary diffusion coefficients are such as to satisfy,

$$\delta_{rs} = \frac{m^2}{m_r m_s} \delta \quad (5-24)$$

where δ , the "overall diffusions function" may be rewritten as,

$$\delta = \left(\frac{m_r m_s}{m}\right) \left(\frac{c_p}{\lambda}\right) D_{rs} \quad (5-25)$$

All flame constituents do not necessarily satisfy this, but (5-24, 25) does at least represent the diffusional behavior of the molecules at least as far as may be expected due to their unequal masses (see subsection 6.2 for a full discussion of this assumption).

The use of the δ -function produces partial linearization of the

diffusion equation,

$$y_r = \left(\frac{m}{\bar{m}}\right) x_r - \left(\frac{m}{\bar{m}_r}\right) \delta \left(\frac{m}{\bar{m}}\right) \left[g \frac{dx_r}{d\tau} - \Gamma_r^E - \Gamma_r^M \right] \quad (5-26)$$

As additional aid in the mathematical solution, the single fluid energy flux is assumed to be everywhere zero (see subsection 6.2 for a full discussion of this assumption). Thus, the defining relationship for the overall diffusion function, δ , is found by eliminating $[y_r - \left(\frac{m}{\bar{m}}\right) x_r]$ from the single-fluid energy flux (i.e. (5-15) set equal to zero) by means of (5-26).

Consequently,

$$\frac{1}{\delta} = -\frac{1}{b} \left(\frac{m}{\bar{m}}\right) \frac{dx_r}{d\tau} \sum_{r=1}^n \left(\frac{m}{\bar{m}_r}\right) \left[L_r - b_r(\tau_\infty - \tau) \right] + \Lambda^E + \Lambda^M \quad (5-27)$$

where,

$$\Lambda^E = \frac{1}{g} \left(\frac{m}{\bar{m}}\right) \frac{1}{b} \sum_{r=1}^n \left(\frac{m}{\bar{m}_r}\right) \left[L_r - b_r(\tau_\infty - \tau) \right] \Gamma_r^E \quad (5-28)$$

$$\Lambda^M = \frac{1}{g} \left(\frac{m}{\bar{m}}\right) \frac{1}{b} \sum_{r=1}^n \left(\frac{m}{\bar{m}_r}\right) \left[L_r - b_r(\tau_\infty - \tau) \right] \Gamma_r^M \quad (5-29)$$

The energy and species equations remain unaltered and will now be written as,

$$a \left(\frac{\bar{m}}{m}\right) = \sum_{r=1}^n \left[L_r - b_r(\tau_\infty - \tau) \right] x_r \quad (5-30)$$

and,

$$\sigma_r = \left(\frac{1}{\alpha b q}\right) g \frac{dy_r}{d\tau} \quad (5-31)$$

In reduced terms, the boundary conditions become:

cold boundary $T = T^0 \Rightarrow T = T_0$

$$g^0 = g(T_0) \cong 0 \quad (5-32)$$

$$\sigma_r^0 = \sigma_r(\dots, x_r^0, \dots, T^0) \cong 0 \quad (5-33)$$

$$x_r^0 \text{ - specified by inlet gas conditions} \quad (5-34)$$

$$y_r^0 = \left(\frac{m}{-m} \right) x_r^0, \text{ r uncharged species; } y_s = 0, \text{ s charged species} \quad (5-35)$$

hot boundary $T = T^\infty \Rightarrow T = T_\infty$

$$g^\infty = g(T_\infty) = 0 \quad (5-36)$$

$$\sigma_r^\infty = \sigma_r(\dots, x_r^\infty, \dots, T_\infty) = 0 \quad (5-37)$$

$$x_r^\infty = \text{determined by the solution of the simultaneous equations (5-37)} \quad (5-38)$$

$$y_r^\infty = \left(\frac{m}{-m} \right) x_r^\infty, \text{ r - uncharged species} \quad (5-39)$$

$$y_s^\infty = 0, \text{ s - charged species} \quad (5-40)$$

6. PROGRAM FOR THE SOLUTION OF THE REDUCED EQUATIONS OF COMBUSTION

6.1 Method of Successive Approximations

The first, and monumental, task is prescribing the kinetic mechanism and accompanying thermodynamic data (heats of formation, and reaction, steric factor, activation energy, specific heat). It is also necessary to know the temperature at the hot boundary and the cold boundary composition. Once known, the solution first requires one to:

- (1) determine x_r^{∞} by the solution of the simultaneous equations (5-37).
- (2) with h_r^{∞} and x_r^{∞} known, the cold boundary temperature can be found from (5-13) with the $g(\tau_0) = 0$, i. e. (5-32). One must be careful that T^0 is sufficiently low such that application of (3-4) confirms (5-33).
- (3) calculate the standard constants (5-1 thru 5-7).

The problem now consists of the simultaneous solution of the equations of energy (5-13), species (5-17) and diffusions (5-21) subject to the hot and cold boundary conditions. The solution sought is one which determines the eigenvalue α , and the variables g , x_r , y_r as functions of the independent variable τ .

Depending on the reaction scheme, considerable simplification can be gained from an a priori order of magnitude analysis of the ion mole fraction. Thus, for a charged species s ,

$$n_s \approx 10^{10} \text{ ions/cc} \quad \Longrightarrow \quad x_s \approx 10^{-7} \quad (6-1)$$

and calculation of the standard constants (5-1 thru 5-7) can be made independently of the ions. Other simplifications will also be obvious upon a further examination of the specific reaction scheme.

It is possible to combine the energy and species equations (5-13,17) into a single nonlinear differential equation involving an unknown eigenvalue. The approximate solutions of this equation and the remaining diffusion equation (5-21) are then used in a method of successive approximations.

Multiplying each species equation by its respective L_r , adding, and employing the energy equation (5-13) in the form,

$$bg = \sum_{r=1}^n L_r y_r - [a + b(\mathcal{T}_\infty - \mathcal{T}) - b\mu_1] \quad (6-2)$$

where,

$$\mu_1 = \frac{\mathcal{T}_\infty - \mathcal{T}}{b} \sum_{r=1}^n [b_r - b \left(\frac{m_r}{m}\right)] y_r \quad (6-3)$$

one obtains,

$$g(1 - \mu_1' - \frac{dg}{d\mathcal{T}}) = \alpha q \sum_{r=1}^n L_r \sigma_r = \alpha q \Omega(\dots, x_r, \dots, \mathcal{T}) \quad (6-4)$$

where μ_1' is the derivative of equation (6-3) with respect to \mathcal{T} . Initially, therefore, it will be necessary to solve this first order, non-linear ordinary differential equation where α is an unknown constant and the boundary conditions are,

$$g(\mathcal{T}_0) = 0, \quad g(\mathcal{T}_\infty) = 0 \quad (6-5)$$

This relation expresses the eigen value problem succinctly, and as in former studies^(9, 35, 38, 39, 40) will be considered the fundamental equation of combustion. A solution is to be found whose detailed structure depends largely on the individual reaction and diffusion

equations. The method of attack will be based in part on that suggested by Klein⁽³⁵⁾ for flames without electromagnetic fields. One assigns lower approximations to the x_r on the right of (6-4) (and \mathcal{U}_1' on the left), and finds by the method of successive approximations estimates to $g(\mathcal{T})$ and to the constant \mathcal{Q} . Once found, g and \mathcal{Q} are used in the remaining equations which, treated "judiciously", serve as definitions for better approximations to the x_r . The process is then repeated until convergence results.

Only a solution of equation (6-3) in the range $\mathcal{T}_0 < \mathcal{T} < \mathcal{T}_\infty$ is of physical interest and the function $\Omega(\mathcal{T})$ is assumed to have the following properties;

(a) in $\mathcal{T}_0 < \mathcal{T} < \mathcal{T}_\infty$ $\Omega(\mathcal{T})$ is never negative,

(b) it is vanishingly small near $\mathcal{T} = \mathcal{T}_0$ and in particular

$$\Omega(\mathcal{T}) = 0, \quad \mathcal{T} \leq \mathcal{T}_0; \quad \left[\frac{d\Omega(\mathcal{T})}{d\mathcal{T}} \right]_{\mathcal{T}_0} = 0$$

(c) $\Omega(\mathcal{T})$ reaches a maximum and vanishes again at $\mathcal{T} = \mathcal{T}_\infty$

It is found⁽³⁵⁾ to be advantageous to consider the solution to equation (6-4) as an integral equation problem, since the boundary conditions will be then contained in the equation itself. The most immediate form in which (6-4) and its boundary conditions can be written in integral form is,

$$1/2 g^2 = \int_{\mathcal{T}_\infty}^{\mathcal{T}} g d\mathcal{T} - \int_{\mathcal{T}_\infty}^{\mathcal{T}} g \mathcal{U}_1' d\mathcal{T} - \mathcal{Q} \int_{\mathcal{T}_\infty}^{\mathcal{T}} \Omega(\mathcal{T}) d\mathcal{T} \quad (6-6)$$

where in order that the boundary conditions are satisfied,

$$\alpha = \frac{\int_{T_0}^{T_\infty} g(1 - \mu_1') dT}{\int_{T_0}^{T_\infty} \Omega(T) dT} \quad (6-7)$$

Once the integral equation has been solved, the above expression for α represents the desired eigenvalue.

Since the required variable g occurs in the integral equation three times, it may be supposed that the integrals are not much affected if slightly incorrect values for g are employed. This being the case, the following scheme for a solution by successive approximations has been

suggested by Klein⁽³⁵⁾

$$g^{(i+1)} = \left(2 \left(\alpha^{(i+1)} \int_T^{T_\infty} \Omega(T) dT - \int_T^{T_\infty} g^{(i)} (1 - \mu_1') dT \right) \right)^{1/2} \quad (6-8)$$

where

$$\alpha^{(i+1)} = \frac{\int_{T_0}^{T_\infty} g^{(i)} (1 - \mu_1') dT}{\int_{T_0}^{T_\infty} \Omega(T) dT} \quad (6-9)$$

The problem has now been separated into two tasks: the eigenvalue α and the accompanying solution of the non-linear differential equation (fundamental equation), and the solution of the remaining equations for x_r and y_r .

In summary, the equations to be solved for an N-species gas are:

$$g(1 - \mu_1' - \frac{dg}{dT}) = \alpha \Omega(\dots, x_r, \dots, T) \quad (6-10)$$

$$\mu_1 = \frac{T_\infty - T}{b} \sum_{r=1}^N \left[b_r - \left(\frac{m_r}{m} \right) b \right] y_r \quad (6-11)$$

$$y_r = \left(\frac{m}{m_r} \right) x_r - \left(\frac{m}{m_r} \right) \left(\delta \frac{m}{m} \right) \left(g \frac{dx_r}{dT} - \Gamma_r^E - \Gamma_r^M \right), \quad (N-1 \text{ relations}) \quad (6-12)$$

$$\Gamma_r^E = \left[\frac{bcE_o^3 [R \lambda(\tau_o)]^{1/2}}{pc_p} \right] q \alpha^{1/2} x_r \left(\frac{m_r}{m} \right) \left(\gamma_r - \sum_{r \neq s=1}^N x_s \left(\frac{m_s}{m} \right) \gamma_s \right) \quad (6-13)$$

$$\Gamma_r^M = \left[\frac{\lambda(\tau_o) q (B_o^2)^2}{pc_p} \right] x_r \left(\frac{m_r}{m} \right) \left(-\gamma_r K_r(T) + \sum_{r \neq s=1}^N x_s \left(\frac{m_s}{m} \right) \gamma_s K_s(T) \right) \quad (6-14)$$

$$\sum_{r=1}^N \left(\frac{m_r}{m} \right) y_r = 1 \quad (6-15)$$

$$\bar{m} = \sum_{r=1}^N m_r x_r \quad (6-16)$$

$$\sigma_r = \frac{1}{\alpha b} g \left(\frac{dy_r}{dT} \right) \quad (N-2 \text{ relations}) \quad (6-17)$$

$$\sum_{r=1}^N x_r = 1 \quad (6-18)$$

$$\sum_{r=1}^N L_r x_r = \left(\frac{\bar{m}}{m} \right) [a + b(T_\infty - T)] + b \mu_2 \quad (6-19)$$

$$\mu_2 = \frac{T_\infty - T}{b} \sum_{r=1}^N \left[b_r - \left(\frac{\bar{m}}{m} \right) b \right] x_r \quad (6-20)$$

$$\Omega = - \sum_{r=1}^N L_r \sigma_r \quad (6-21)$$

$$\left(\frac{\bar{m}}{m}\right) \frac{1}{\delta} = -\frac{1}{b} \frac{d}{d\tau} \left[\sum_{r=1}^N \left(\frac{m}{m_r}\right) L_r x_r \right] + \mu_3 + \Lambda^E + \Lambda^M \quad (6-22)$$

$$\mu_3 = \frac{\tau_\infty - \tau}{b} \frac{d}{d\tau} \left[\sum_{r=1}^N \left(\frac{m}{m_r}\right) b x_r \right] \quad (6-23)$$

$$\Lambda^E = \frac{1}{g} \left(\frac{m}{\bar{m}}\right) \frac{1}{b} \sum_{r=1}^N \left(\frac{m}{m_r}\right) [L_r - b_r(\tau_\infty - \tau)] \Gamma_r^E \quad (6-24)$$

$$\Lambda^M = \frac{1}{g} \left(\frac{m}{\bar{m}}\right) \frac{1}{b} \sum_{r=1}^N \left(\frac{m}{m_r}\right) [L_r - b_r(\tau_\infty - \tau)] \Gamma_r^M \quad (6-25)$$

A detailed method of successive approximations will not be presented. It must be remembered that E_o^3 and B_o^2 are known values.

- (1) Let $x_r(\tau)^{(1)}$ be assumed approximations to x_r satisfying (6-18, 19) and $\mu_2^{(1)} = 0$. With these $x_r^{(1)}$, approximations to $\Omega(\tau)^{(1)}$ and $\frac{m}{\bar{m}}(\tau)^{(1)}$ can be made from (6-21, 16). For the lowest approximation $\left(\frac{\bar{m}}{m} \frac{1}{\delta}\right)^{(1)}$ can assumed to be unity.
- (2) A preliminary function $g(\tau)^{(0)}$ possessing the expected characteristics of the final $g(\tau)$ is next arbitrarily assumed.
- (3) With $\Omega(\tau)^{(1)}$, $g(\tau)^{(0)}$ and $\mu_1^{(0)} = 0$, one can by (6-8, 9) determine a new function $g(\tau)^{(1)}$ and the eigenvalue $\alpha^{(1)}$.
- (4) With the $g(\tau)^{(1)}$ so obtained and with the quantities of steps (1, 3), one now calculates approximations $y_r(\tau)^{(1)}$ from (6-12, 13, 14, 15, 16). Note y_r , $r = 1, 2, \dots, N - 1$, are

determined by (6-12,13,14), and y_N by (6-15). The selection of which is the N-th species is the individual's prerogative based on knowledge and behavior of the chemical kinetics.

- (5) From these $y_r(\mathcal{T})^{(1)}$ and $\alpha^{(1)}$, $g(\mathcal{T})^{(1)}$, one finds (from 6-17) as functions of \mathcal{T} , better approximations than those used in step (1) for the production rates $\sigma_r(\mathcal{T})^{(2)}$, $r = 1, 2, \dots, N-2$. Again the selection of which two of N species to ignore is a matter of prerogative.

- (6) One now calculates better approximations $x_r(\mathcal{T})^{(2)}$ by the solution of the simultaneous algebraic, but often nonlinear, equations

$$\sigma_r(\dots, x_r^{(2)}, \dots, \mathcal{T}) = \sigma_r^{(2)}(\mathcal{T}), \text{ [from step 5]}$$

and equations (6-18,19) with $\mu_2^{(2)} = f(\mathcal{T}, x_r^{(1)})$.

- (7) With $x_r(\mathcal{T})^{(2)}$, the quantities $\Omega(\mathcal{T})^{(2)}$, $\frac{m}{\bar{m}}(\mathcal{T})^{(2)}$, $\mu_3^{(2)}(\mathcal{T})$, $\Gamma_r^E(\mathcal{T})^{(2)}$, $\Gamma_r^M(\mathcal{T})^{(2)}$, $\Lambda^M(\mathcal{T})^{(2)}$, $\Lambda^{E^m}(\mathcal{T})^{(2)}$ are found from (6-13,14, 21, 22, 23, 24, 25).
- (8) From $g(\mathcal{T})^{(1)}$, $\Omega(\mathcal{T})^{(2)}$, $\mu_1^{(2)} = f(y_r^{(1)}, \mathcal{T})$, the function $g(\mathcal{T})^{(2)}$ and eigenvalue $\alpha^{(2)}$ are found from (6-8, 9).
- (9) With these newly found $g(\mathcal{T})^{(2)}$ and the quantities of step (7), one now calculates new $y_r(\mathcal{T})^{(2)}$ from (6-12,15).
- (10) From these $y_r(\mathcal{T})^{(2)}$, $\alpha^{(2)}$, $g(\mathcal{T})^{(2)}$, one finds (from 6-17) as functions of \mathcal{T} , better approximations than those used in step (8) for the production rates $\sigma_r(\mathcal{T})^{(3)}$, $r = 1, 2, \dots, N-2$.

- (11) One now calculates better approximations $x_r(\mathcal{T})^{(3)}$ by the solution of the simultaneous equations,

$$\sigma_r(\dots, x_r^{(3)}, \dots \mathcal{T}) = \sigma_r^{(3)}(\mathcal{T}), \text{ [from step 10]}$$

and equations (6-18,19), with $\mu_2^{(3)} = f(\mathcal{T}, x_r^{(2)})$.

- (12) With the newly found $x_r(\mathcal{T})^{(3)}$, steps 7 thru 11 are repeated until satisfactory convergence results.

6.2 Discussion

The terms μ_1, μ_2, μ_3 (Eqs. 6-11, 20, 23) represent perturbations for which only the inequality of the specific heats of the components is responsible. As they are zero at the boundaries, the boundary conditions will not be affected by neglecting them all together on the first approximation, and in the method of successive approximations it will be possible to always express them in terms of lower approximations of the x_r and y_r .

Comments by Klein⁽³⁵⁾ will be inserted here as they throw light on the convergence of the proposed method.

- (1) It is not implied that the scheme is genuinely convergent everywhere on the temperature range or for all possible forms of the rate constants; even if convergence could be proved for certain ranges $\left| x_r^{(0)} - x_r \right|$, it is unlikely that one will fortuitously choose a suitable lowest approximation. The scheme, as it stands, represents, therefore, on the one extreme, a perfect guide to the solution, involving genuinely converging approximations; and on the

otherhand, a mere rule by which certain "input" quantities $x_r^{(i)}$ may be made to produce certain "output" quantities $x_r^{(i+1)}$.

- (2) A numerical solution only as close as desired to the actual solution is all that is required. It can generally be attained by schemes such as

$$x_r^{(i)} = 1/2 [x_r^{(i)} + x_r^{(i-1)}] \quad (6-26)$$

- (3) An excellent criterion for the overall convergence of the scheme are successive values of $\alpha^{(i)}$ since estimation of the flame speed is often of principle interest. From $\alpha^{(i)}$ the flame speed can be found,

$$S_u^2 = \left[\frac{1}{b^2} \left(\frac{\lambda(T_o)}{R} \right) \frac{RT_o}{p} \right] \frac{1}{\alpha} \quad (6-27)$$

- (4) Application of scheme similar to the above but where there were no electromechanical fields reported⁽³⁵⁾ satisfactory convergence in about 10 trials.

The diffusion equations for a multicomponent gas are so complex that contemporary studies^(9, 35, 38, 71, 72) customarily use approximate relationships for the diffusion velocities and diffusion coefficients.

The assumption of zero energy flux (4-25) and the overall diffusion coefficient (5-24, 25) are phenomenologically related and restrict the class of chemical reactions that can be considered. A zero energy flux implies that for each volume element, an equal amount of energy is added by thermal conduction as is removed by diffusion. It is a

simple matter to show that this assumption is equivalent to assuming that the enthalpy is everywhere constant. In terms of transport coefficients, it means that energy transport by thermal conduction and diffusion balance. For a binary mixture, this is equivalent to saying the Lewis number,

$$L_e = \frac{\lambda}{c_m c_p D_{ij}} \quad (6-28)$$

is unity. For binary mixtures and unimolecular reactions ($A \rightarrow B$), this is easily interpreted, but for multicomponent mixtures this is not the case. Spalding⁽⁹¹⁾, Hirschfelder⁽²⁾, von Karman⁽³⁸⁾, and others⁽⁷⁴⁾, have employed a unity Lewis number to several known flames of binary mixtures (i.e. hydrazine decomposition) with considerable success. Consequently, von Karman suggests the constant enthalpy process is a useful concept as a first approximation for general reactions concerning an n-species gas.

The overall diffusion coefficient, δ , imposes some restriction on the characteristics of diffusion, but particularly on the molecular weights of the chemical species in the combustion reaction. In an illuminating contribution, Hirschfelder⁽⁷⁹⁾ demonstrated that when the enthalpy is constant, the multicomponent diffusion coefficients must satisfy,

$$D_{ij} = \left(\frac{\lambda}{c_p m c_{m_j}} \right) \left(m + (m_j - m_i) x_i \right) \quad (6-29)$$

Consequently, Klein's assumption that the diffusion function, δ , be independent of species requires that,

$$\frac{1}{\delta} = \left(\frac{m}{m_i} \right) / \left(m + (m_j - m_i) x_i \right) \quad (6-30)$$

be constant, or at worst a function of temperature. Compatibility with Hirschfelder⁽⁷⁹⁾ is achieved if the mass ratio of all species is roughly one. This being so, the Lewis numbers for any pair of species is also one, and the binary diffusion coefficients are the same or nearly so and related by,

$$\frac{D_{ij}}{D_{st}} = \frac{m_s m_t}{m_i m_j} \quad (6-31)$$

The method of successive approximations was not pursued beyond this point because of computer storage limitations and inadequate knowledge of the chemical kinetics of chemionization.

When the previous analytical method was developed, the Control Data Corporation Model 3600 computer was not in operation. The limited storage capacity of the existing machines required that the method of successive approximations had to be divided into several sections, the output from one section acting as input to the next. The time required to obtain a satisfactory solution was considered to be excessive and it was suggested that it not be attempted.

While the three chemical reactions described in Section 2.2 best describe the probable formation of the major flame ions in the luminous portion of a flame, they are by no means inclusive. The present state of combustion science has not progressed to the point where a reaction mechanism describing the formation of combustion species (charged

and uncharged) from the hot to the cold boundary has been proposed. Not having such information, and rather than inventing a reaction of little practical importance; it was decided it would be more profitable to develop an approximate theory which described the flame-field interaction and to confirm such a theory by experiment.

7. AN APPROXIMATE THEORY - CHATTOCK ELECTRIC WIND

The primary effect of an electric field is to modify the velocities and directions of the "thermal trajectories" of the ions during each mean free path in such a way as to increase the velocity component in the direction of the field. The additional momentum in the field direction of an ion before each equilibrating collision is $Ee\Delta t$, where Δt is the time between collisions. If this quantity is small in comparison with the "thermal momenta" of the ions, the time between collisions will not differ appreciably from those in the absence of the field and the proportionality of drift velocity and electric field strength exists. When the ion has obtained equilibrium, the additional energy is lost to the gas molecules during collisions. The subsequent fate of this energy depends on whether the collisions are elastic or inelastic.

In inelastic collisions, which are possible if the induced energy is high enough, the energy may give rise to secondary ionization or to excitation within any one of the other degrees of freedom of the target molecule, ultimately to be radiated out of the system or degraded to thermal energy. The result of such a collision does not contribute directly to the body force (although in the case of secondary ionization it may do so indirectly by increasing the ion concentration).

If the collisions are elastic, the additional momentum in the direction of the field is conserved and results in a body force on the gas, which since the ion does not continue to accelerate, is identical in magnitude to that which would be expected if ions were rigidly fixed

with respect to the body of the gas.

While suffering from a lack of rigor, the application of the Chattock electric wind offers much in the way of clarity and simplicity.

In this regard, the following assumptions will be made:

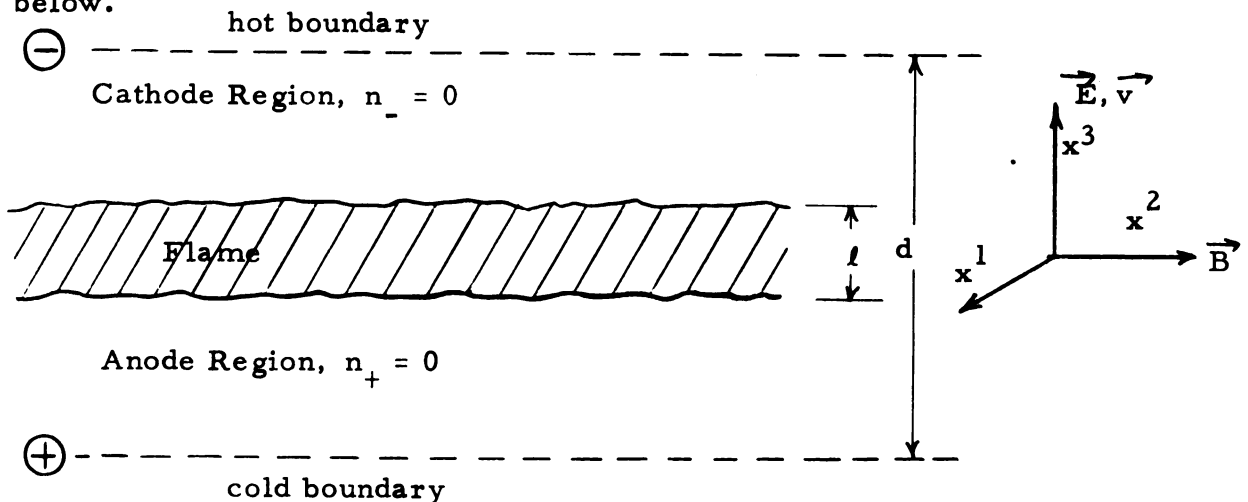
- (1) single-species, continuum, inviscid gas obeying the perfect gas equation of state
- (2) flame consists of a discrete plane layer of thickness l
- (3) constant electric and magnetic field (E^3, B^2)
- (4) force per unit volume representable by the Lorentz equation

$$\vec{X} = n e [\vec{E} + \vec{u} \times \vec{B}] \quad (7-1)$$

- (5) electron-molecule momentum transfer is negligible
- (6) diffusion is negligible

To isolate the electromagnetic effects, consider the steady flow of a gas and a two dimensional ion-generating layer of thickness l , embedded between two parallel electrodes with an orientation as shown

below.



Normal flame in a one-dimensional flow - Positive electric field

Fig. 7-1

From experiments with Langmuir probes, it is known that adjacent to each electrode one can expect a sheath of charge of opposite polarity⁽⁵⁸⁾. Thus adjacent to the anode is a layer of electrons which owing to their large mobility is very thin (as compared to a charge layer near the cathode). If other negative ions are stable at anode temperatures, one can expect equilibrium concentrations of these in addition to the electrons, however only electrons have been observed to date⁽⁶⁸⁾. Within the anode layer, the voltage gradient is very steep.

Adjacent to the cathode is a layer of positive charges. Positive ions are large atom complexes (radicals or molecular ions) and the charge density is primarily governed by the temperature and thermodynamic equilibrium. The positive ions observed in flames are not stable at low temperatures (even the temperatures of the hot boundary) and consequently, the cathode charge layer is thought to be unimportant unless a significant amount of "seeding" is done. Adding a material to the gas which possesses a low ionization potential, i.e. alkali metals (Na, K, Rb, Cs) results in thermal ionization of that material as it passes through the flame. In the case of alkali metals, the positive ions so formed migrate to the cathode and reside for a time in its vicinity. The equation governing the concentration is the Saha equation (2-1) and a significant concentration of positive ions can only occur if the cathode temperature and the initial seeding rates are sufficiently large.

If diffusion as a consequence of concentration gradients is ignored

the positive and negative ions would drift in opposite directions as soon as they are formed in the flame. Thus neglecting secondary ionization, $n_- = 0$ in the cathode region and $n_+ = 0$ in the anode region.

In both the anode and cathode regions E and n may vary in a continuous fashion. The true nature of E and n can be found by solving Maxwell's equations with known boundary conditions on n , \vec{J} , \vec{B} , \vec{E} . Solution of these equations is difficult and at best involves estimates of n_+ , n_- in the flame and at the boundaries. It is possible to side step estimates of ion densities by employing experimentally measurable current densities, \vec{J} . In steady state, \vec{J} is constant in regions where no ions are generated,

$$\begin{aligned} \vec{J} &= e[n_+\vec{u}_+ - n_-\vec{u}_-] \\ &= e\vec{E}[n_+K_+ - n_-K_-] = \text{const.} \end{aligned} \quad (7-2)$$

Expansion of (7-1) indicates that x^3 forces arise from the magnetic field and the transverse ion velocities u_+^1 , u_-^1 .

The velocity u^1 is the transverse drift velocity arising from $(u^3 B^2)$ and is commonly called the "Hall effect". Such currents are small, but in the configuration, Fig. 7-1, may be important since they enter into the calculation of force due to the magnetic field.

In an electric field, the force on a positive ion is Ee and this force causes a velocity K_+E . The velocity of a positive ion due to a unit force is then K_+/e . In a similar fashion, the velocity per unit force on a negative ion is $-K_-/e$ (note the mobility is signed). The transverse force on a positive ion is,

$$f_+^1 = -e u_+^3 B^2 = -e B^2 (K_+ E^3) \quad (7-3)$$

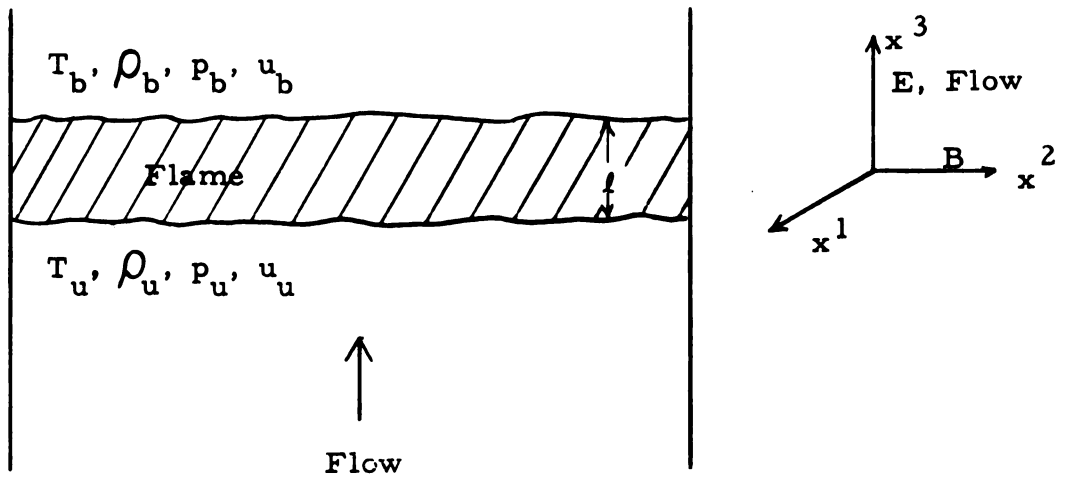
and from the above, the velocity in the x^1 direction is

$$u_+^1 = v_+^1 = f_+ \left(\frac{K_+}{e} \right) = -K_+ u_+^3 B^2 = -K_+ B^2 (K_+ E^3) \quad (7-4)$$

The upward force per unit volume due to the positive ions is,

$$\begin{aligned} X_+^3 &= f_+^3 n_+ \\ X_+^3 &= e n_+ [E^3 - v_+^1 B^2] \\ X_+^3 &= e n_+ E [1 + (BK_+)^2]^* \end{aligned} \quad (7-5)$$

Consider the following one-dimensional flow situation



Normal flame in a one-dimensional flow - Positive electric field

Fig. 7-2

The following simplified conservation equations apply. ⁽⁴⁾

continuity

$$\rho_b u_b = \rho_u u_u \ddagger \quad (7-6)$$

* the superscripts on \vec{B} and \vec{E} have been removed for simplicity, i.e.

$E^3 = E$, $B^2 = B$.

‡ the superscripts b, u refer to the conventional "burned" and "unburned" states.

energy

$$\Delta h = c_p (T_b - T_u) + \frac{\rho_b u_b^2}{2} - \frac{u_u^2 \rho_u}{2} \approx c_p (T_b - T_u)$$

$$N \equiv T_b / T_u = 1 + \frac{\Delta h}{c_p T_u} \quad (7-7)$$

state

$$p_b = \rho_b R T_b, \quad p_u = \rho_u R T_u \quad (7-8)$$

momentum

$$p_u - p_b = \rho_u u_u (u_b - u_u) + X_+ l \quad (7-9)$$

It is convenient to define the flame speed (S_u) thru the following,

$$\iint_{A_1} \rho \vec{u} \cdot d\vec{A} = \iint_{A_f} \rho \vec{S}_u \cdot d\vec{A} \quad (7-10)$$

where A_1 is at any appropriate point and A_f is conveniently taken as the visible surface area on the "unburned" side of the flame. From Fig. 7-2, it is seen that the flame speed is equal to u_u . Thus

$$(p_u - p_b) = \rho_u S_u (u_b - u_u) + X_+ l \quad (7-11)$$

For gases, the density decrease depends primarily upon the temperature increase, with a small additional effect for the change in composition. The velocity change then follows from the continuity equation

$$\frac{u_b}{u_u} = \frac{\rho_u}{\rho_b} = \left(\frac{p_u}{p_b} \right) \left(\frac{T_b}{T_u} \right) \approx \frac{T_b}{T_u} = N \quad (7-12)$$

Thus,

$$(u_b - u_u) = S_u (N - 1) \quad (7-13)$$

which allows one to write,

$$S_u = \left(\frac{(p_u - p_b) + Ee n_+ \ell [1 + (BK_+)^2]}{(N - 1) \rho_u} \right)^{1/2} \quad (7-14)$$

A vast amount of knowledge concerning the flame speed without fields (S_u^o) has been gained, and if one reapplies the previous equations without a field, the quantity $(p_u - p_b)$ can be eliminated from (7-14).

Thus,

$$S_u = \left((S_u^o)^2 + \frac{Ee n_+ \ell [1 + (BK_+)^2]}{(N - 1) \rho_u} \right)^{1/2} \quad (7-15)$$

To appreciate the manner in which electric and magnetic fields effect the flame speed, consider Fig. 7-3 which represents the flame speed as a function of the electric field intensity (7-15) for flames with two different ion populations (n_+ , ions/cc), and positive and negative electric fields. A flame with the following representative properties will be assumed,

$$\begin{aligned} S_u^o &= 60 \text{ cm/sec} & K_+ &= 2.85 \text{ volt sec/cm}^2 \\ \ell &= 10^{-2} \text{ cm} & \rho_u &= .858 \times 10^{-3} \text{ gm/cc} \\ & & N &= 8 \end{aligned}$$

If the magnetic field exerts a force on the flame solely because of the Hall currents (as has been assumed in this study) equation (7-15) reveals that the effect is extremely small. Once an electric field (E) exists, the magnetic field effects enter through the term, $[1 + (K_+ B)^2]$.

If the magnetic field assists the electric field by even as little as 1%, i.e.,

$$[1 + (K_+ B)^2] = 1.01$$

a magnetic field of 3.7×10^6 gauss will be required. Since the magnetic effects are too small and the associated magnetic fields too large for experimental investigation, further consideration of magnetic fields will be abandoned.

Fig. 7-3 reveals the great influence the ion density has upon (7-15). Extensive experiments (61, 64, 65, 66, 68) in which flames have been probed, and species analyzed by the mass spectrometer have done much to improve an understanding of n_+ and its variation with fuel-air ratio and other combustion parameters, but an a priori prediction of the ion density is seldom better than an order of magnitude.

Equally as difficult to predict is the electric field intensity (E), since adjacent to each electrode are sheaths of positive ions (at anode) and negative ions (at cathode). Thus the effective potential difference which produces the electric field is substantially less than that based on the applied voltage. Lastly, the voltage gradient between the electrodes and in the flame is not necessarily constant.

It is possible to circumvent some of these difficulties by using direct measurements of current and information of flame speed and N as functions of the fuel-air ratio. At any fuel-air ratio, S_u^0 and N are known. Similarly, K_+ and ρ_u can be predicted. Approximate values of the flame thickness, l , are known, but with less accuracy than any of the above terms. As the magnetic effects are of minor importance, a constant value equal to the external field may be assumed with little difficulty. Values for n_+E can be found from experimental

Effect of Electric Field Intensity upon Flame Speed

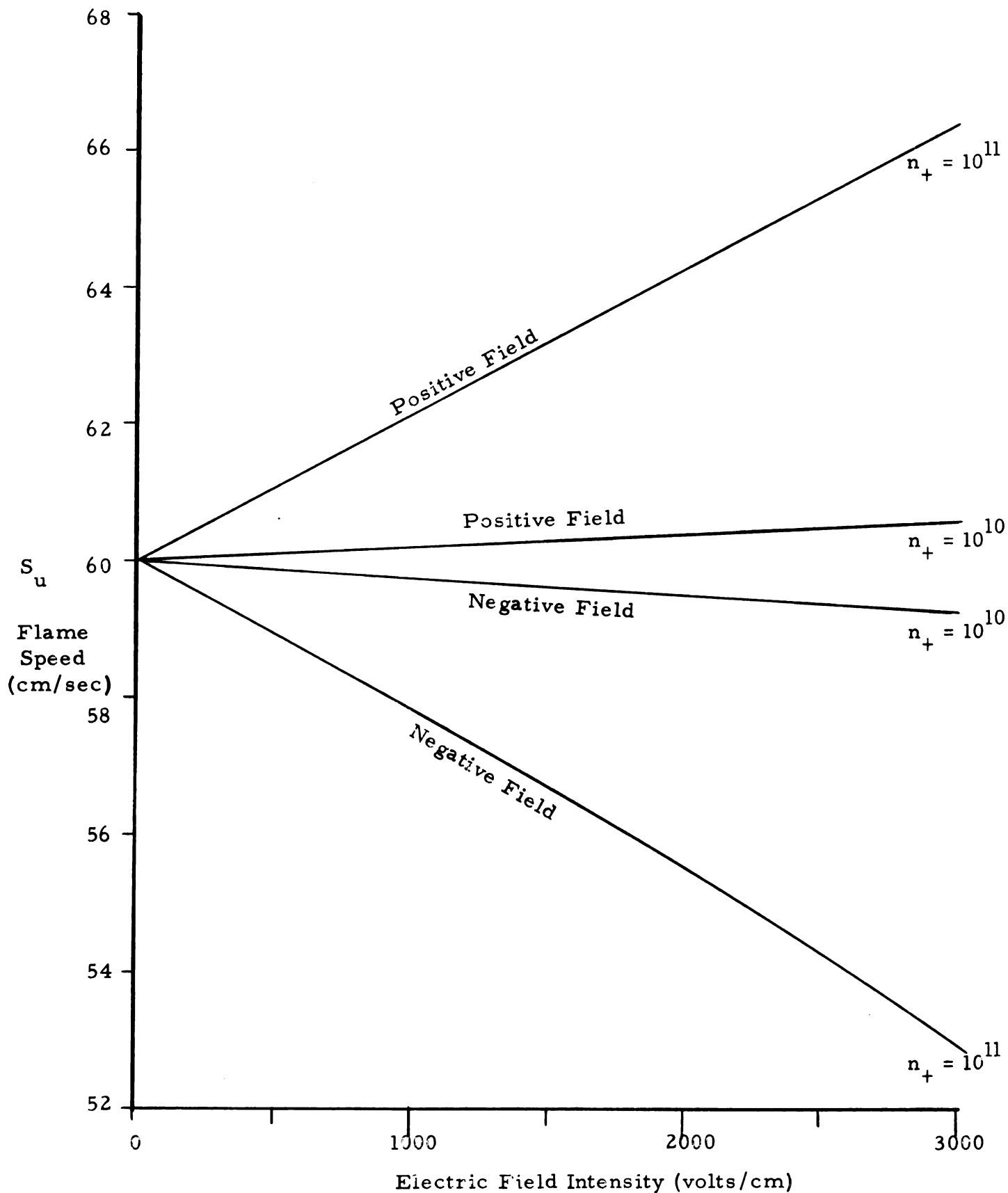
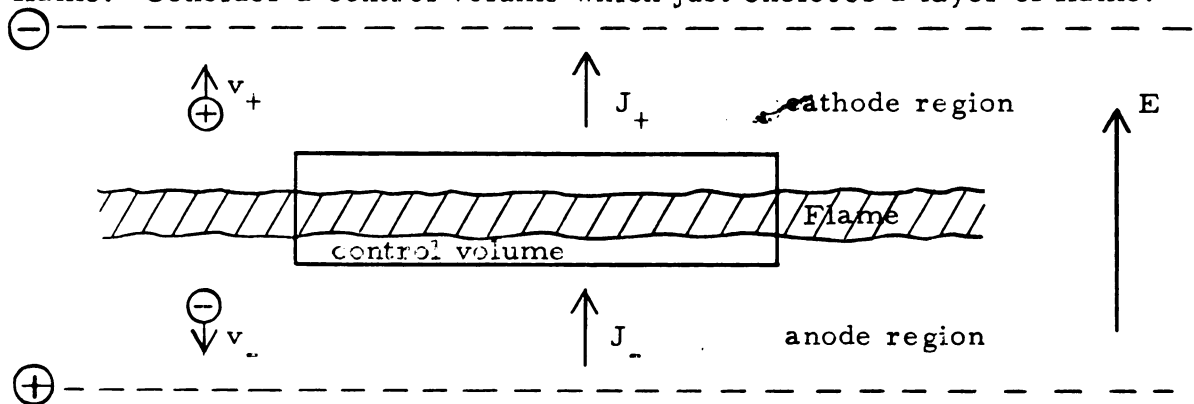


Fig. 7-3

measurements and an appreciation of the chemistry accompanying the flame. Consider a control volume which just encloses a layer of flame.



Normal flame in a one-dimensional flow - Positive electric field

Fig. 7-4

In steady state, continuity of charge requires that,

$$\oint \vec{J} \cdot d\vec{A} = 0 \quad (7-16)$$

such that at the flame surface,

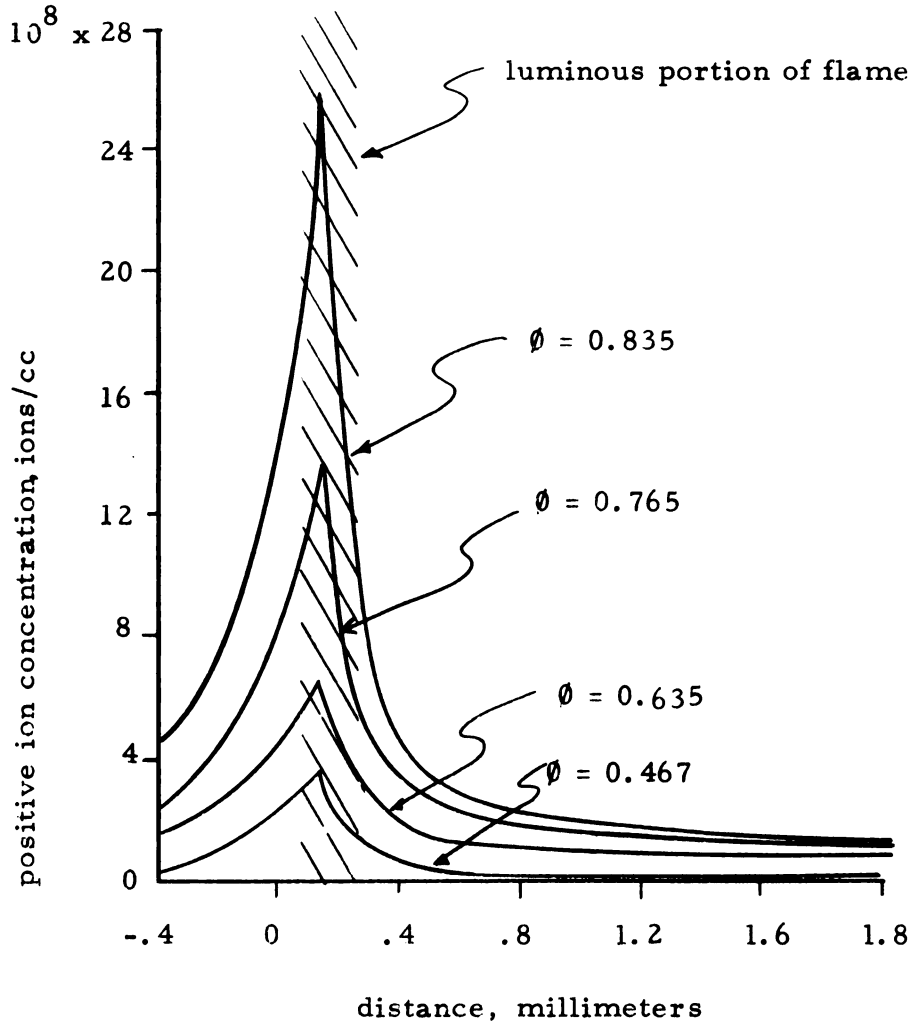
$$J_+ = J_- \quad (7-17)$$

While the cathode region is appreciably hotter than the anode region, the temperature at the cathode is considerably less than in the flame itself. This is particularly true for the lean flames under consideration. The positive ion density at the cathode is consequently considerably less than in the flame itself (by approximately a factor of 10^4) since the positive ions are comprised of,

(a) alkali metal ions which result from seeding and owe their ionization to a high temperature via the Saha⁽⁴⁹⁾ equation (2-1).

(b) positive flame ions (mainly H_3O^+) which are thermodynamically unstable at temperatures below that of the flame.

The above assumptions are supported by King and Calcote⁽⁴³⁾ and their traverses of unseeded propane-air flat flames using the Langmuir probe. Figure 7-5 shows the result of such traverses and in addition demonstrates the keen dependence the fuel-air composition has upon the ion density.



Positive ion concentration through a lean propane flame front as a function of distance. Equivalence ratio (ϕ) varied by diluting air with nitrogen. Flat flame burner at one atmosphere. ⁽⁴³⁾

Fig. 7-5

Thus,

$$J_+ (\text{at the flame}) \gg J_+ (\text{at the cathode}) \cong 0$$

(7-18)

The negative ions comprising J_- are predominately electrons. Due to the high mobility of electrons and their independence of the cold temperatures at the anode,

$$J_-(\text{at the flame}) \cong J_-(\text{at the anode}) \quad (7-19)$$

As a result of the above, it is reasonable to assume that the measured current (I) divided by the area of the flame (A_f) is equal to

$$I/A_f = \left(J_+ \right)_{\text{at cathode}} + \left(J_- \right)_{\text{at anode}} \cong \left(J_- \right)_{\text{at anode}} = \left(J_- \right)_{\text{at flame}} \quad (7-20)$$

As a result of (7-17), (7-20) becomes

$$I/A_f = \left(J_+ \right)_{\text{at flame}} = (en_+ EK_+) \quad (7-21)$$

Solving the above for (En_+) , (7-14) becomes

$$S_u = \left[(S_u^0)^2 + \frac{Il}{A_f K_+ (N-1) \rho_u} [1 + (BK_+)^2] \right]^{1/2} \quad (7-22)$$

8. EXPERIMENTAL TECHNIQUE AND EQUIPMENT*

8.1 Burner

The flat flame burner, Fig. 8-1, was similar in construction to that developed by Powling^(81,82,83,86). Excellent mixing, control, and uniform velocities were achieved. A schematic drawing and photograph of the experimental apparatus is shown in Fig. 8-1, 2, 3. The distance between the upper grid and matrix was 1.25" in all experiments. The fuel used in all experiments was city gas (basically CH₄ and C₂H₆) and air was supplied by a centrifugal blower. Fuel and air flows were measured in positive displacement meters and timed by electric timers. Temperatures at the exit plane of the matrix were recorded by copper-constant on thermocouples. The burner matrix consisted of alternate layers of flat copper strip (.003" x 1") and corrugated copper strip (.003". 1") wound one upon the other until an overall diameter of 3 1/2 inches was obtained. When wound together, the matrix consisted of a great number of small channels with triangular cross section approximately 1/16" x 1/16" x 1/16". Mists were produced by secondary air at 90 psia passing through a commercial perfume atomizer inserted inside a large collecting bottle. Secondary air was metered by a calibrated rotometer.

8.2 Electrostatic Field

Between the upper grid and matrix, an electrostatic field was produced by a high-voltage power supply. Voltages and currents were

* Reference Appendix A for specific details of the equipment used.

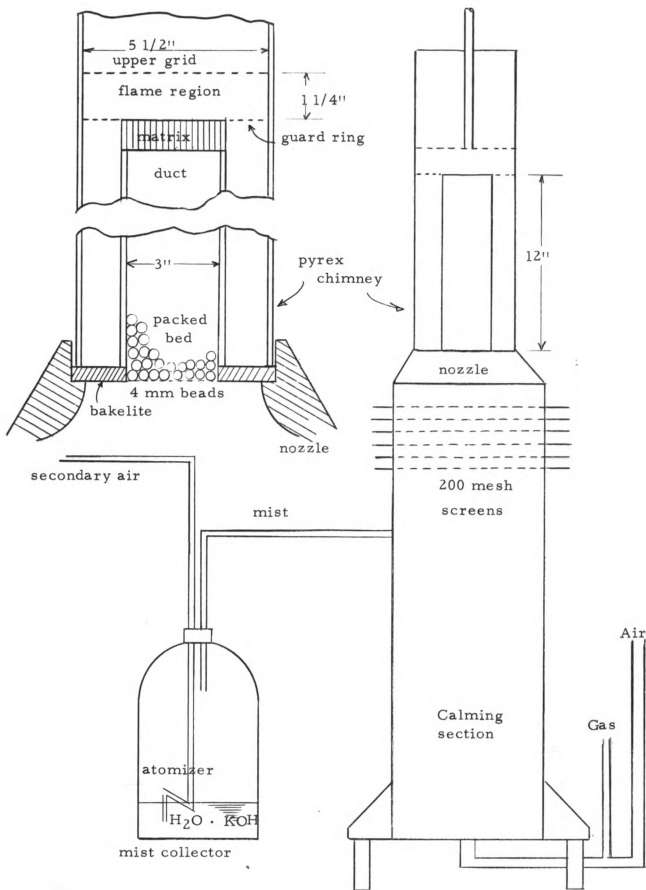


Fig. 8-1

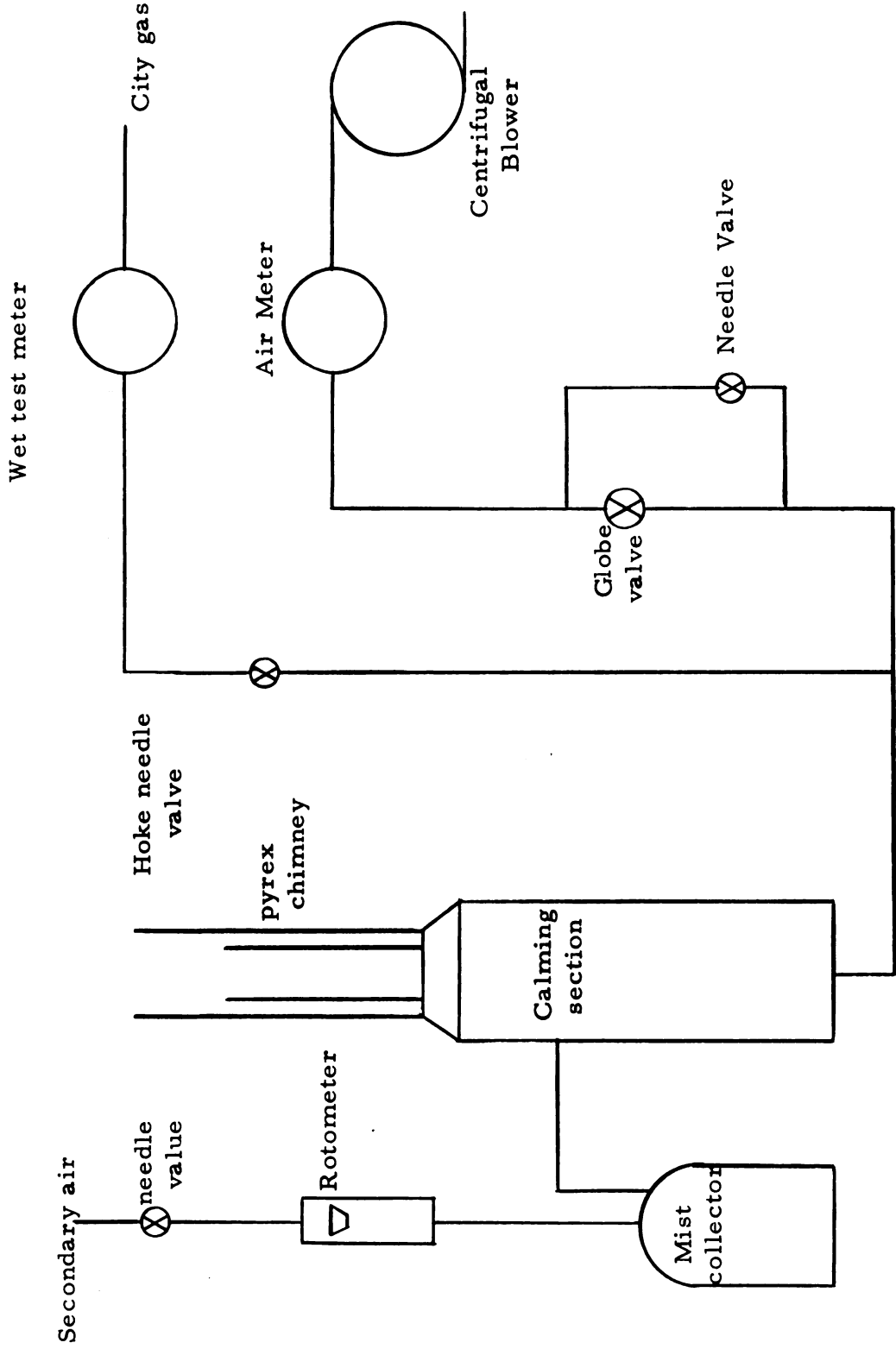
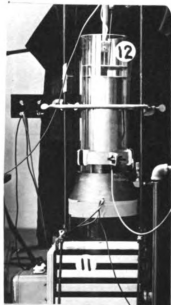
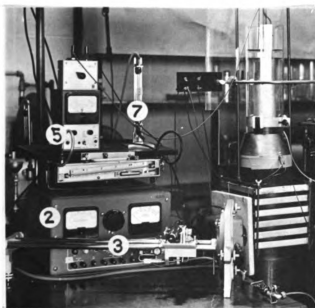
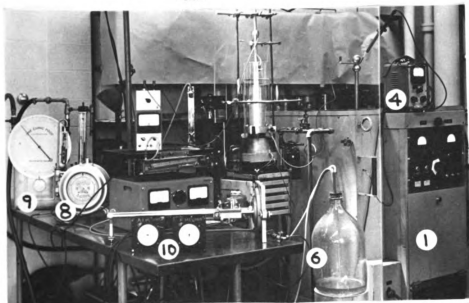


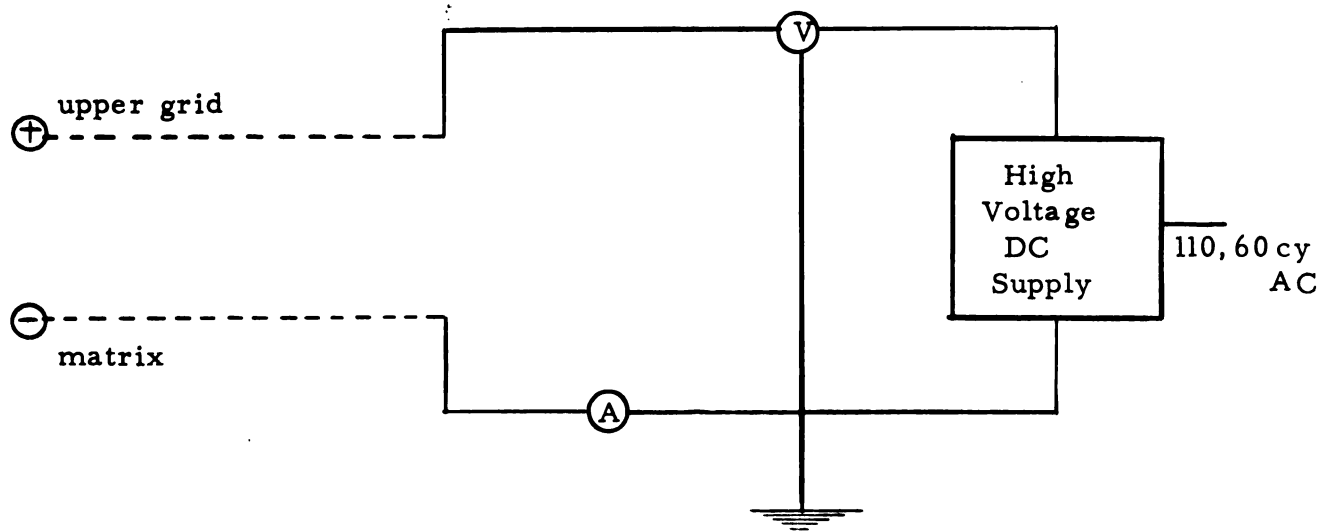
Fig. 8-2



- (1) High voltage power supply
- (2) Low voltage power supply
- (3) Cathetometer
- (4) Voltmeter
- (5) Ammeter
- (6) Mist collector
- (7) Rotometer
- (8) Gas meter
- (9) Air meter
- (10) Timers
- (11) Calming screens
- (12) Pyrex chimney containing duct, upper grid and matrix

Fig. 8-3

measured directly as shown in Fig. 8-4.



Negative Electric Field
Fig. 8-4

8.3 Photography

All photographs were taken at f 5.6 using Royal Pan Film. Flame pictures were made by a double exposure, the equipment under flood light at .1 sec and the flame with no lighting at 1 sec.

8.4 Experimental Technique

Flame extinction experiments were conducted by first obtaining flat flames at particular values of fuel flow, voltage and mist flow and then increasing the air flow until extinction occurred. Flames were studied over a wide range of voltages, lean fuel-air ratios and duct exit velocities. In all cases, the mist flow was constant. The air and fuel flows were corrected for water vapor.

An aqueous potassium hydroxide solution (8.38% KOH, mole fraction) was used throughout all experiments. The air flow used to form a mist was also constant (2.245 li/min) and introduced into

the flame 4.77×10^{-3} gm KOH/min and 1.67×10^{-2} gm H₂O/min.

The later quantities were calculated by bubbling the mist at a constant rate through a gas dispersion tube emmersed in a standard HCl solution and timing the color change of phenolphthalein.

9. EXPERIMENTAL RESULTS

9.1 Bunsen Burner Flames

A graphic demonstration of the distortion of a flame by an electric field is seen in Fig. 9-1. The electric field was produced by two charged stainless steel screens (1 3/8" x 3 3/8") normal to the photograph. At maximum voltage, the concave side of the flame was progressively flatter as one approached the flame tip. The normally conical flame took on the shape of a wedge arched toward the cathode. The flame tip was approximately 1/4" wide. No attempt was made to analyze these flames as the peculiar geometry and distorted streamlines seriously hamper analysis⁽¹²⁾. All flames deflected toward the cathode in agreement with the findings of Weinberg^(55, 53) and Calcote^(11, 12).

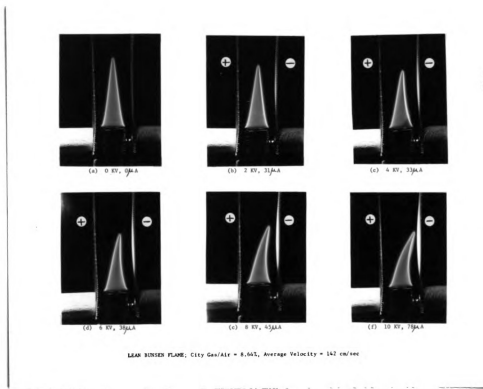
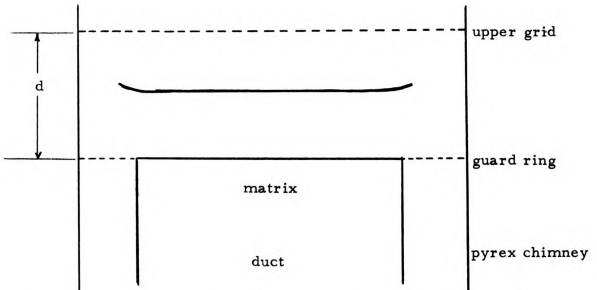
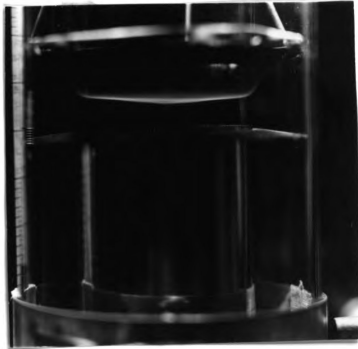


Fig. 9-1

9.2 Flat Flames without Seeding

A typical flat flame in the absence of electromagnetic fields and seeding is seen below,



Average gas velocity = 17.2 cm/sec

Fuel-air ratio = 4.82%

Typical Unseeded flat flame without an electric field

Fig. 9-2

Stable flames have diameters slightly larger than the burner and are suspended between the matrix and downstream grid. The vertical position of the flame is governed principally by the distance d , but is essentially midway between the grid and matrix. The stable flame displays a slightly convex center (with respect to the on coming flow) and a curved lip at its periphery, nevertheless the flame sheet is substantially flat over the major portion of its surface. Stable flames were obtained for duct velocities from 5 to 20 cm/sec. The flames of interest were below 15 cm/sec since the flame sheet is more flat and lip less curved at lower gas velocities.

While a transverse electric field easily distorts a bunsen flame, a flat flame experiences only slight changes in position and diameter when subjected to an axial electric field. In order to determine why the unseeded flat flame is virtually insensitive to electric fields, while bunsen flames are easily deflected, a series of experiments were conducted in which current and applied voltage were measured at constant duct velocity and fuel-air ratio. The results of these tests are shown in Fig. 9-3. At any voltage, the current is seen to increase with fuel-air ratio. It should be noted that while the duct velocity remained constant at about 16 cm/sec, only the flame with a fuel-air ratio of 5.08% was flat, the other flames were attached to the matrix in a manner similar to a laboratory Meeker burner.

Lean bunsen flames readily distort at a fuel-air ratio of 8.65% and at such values Fig. 9-3 reveals that the current, hence ion density,

Current vs Voltage of Constant Fuel-Air Ratio* for
Unseeded Flames

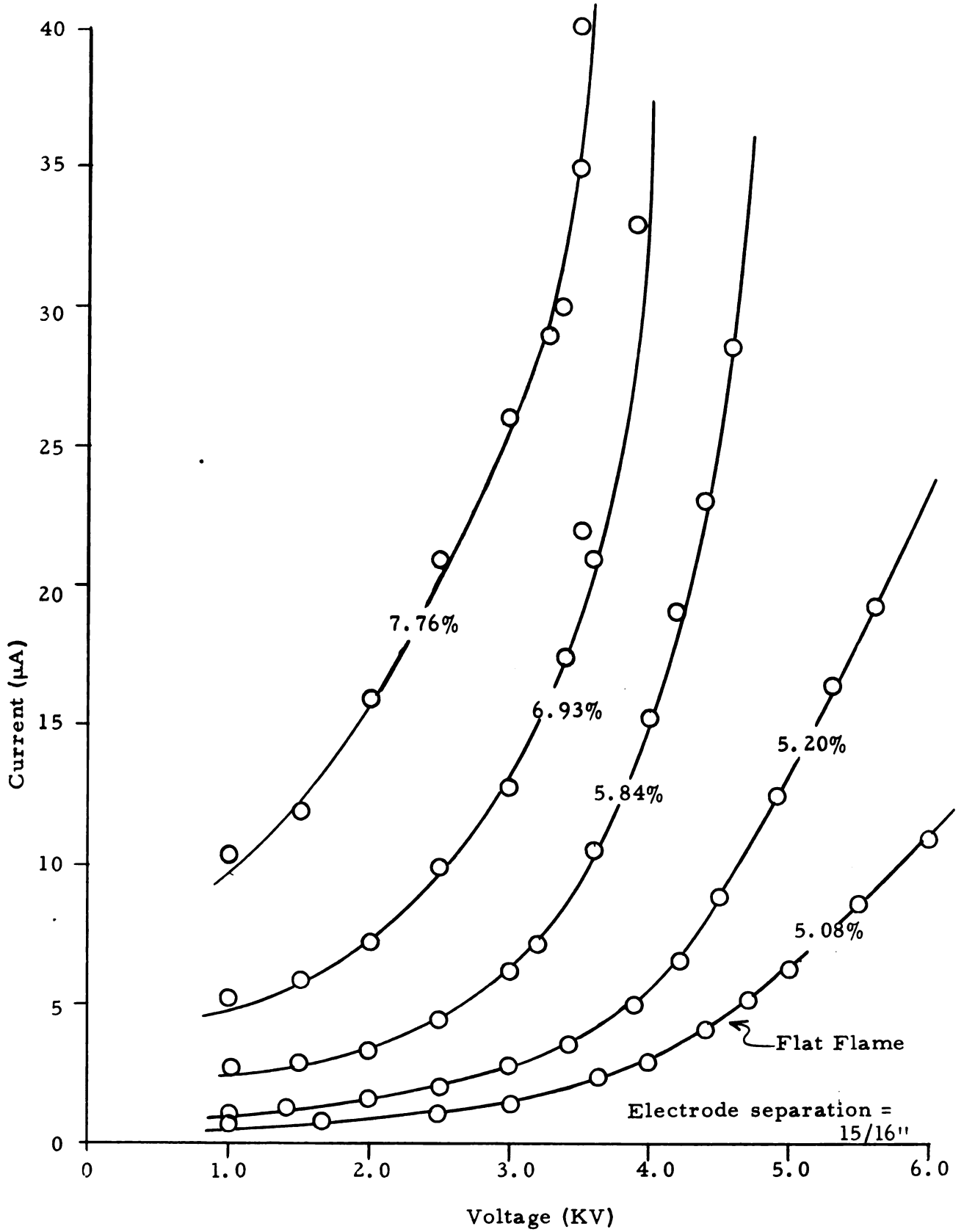


Fig. 9-3

is more than ten times that of the flat flame. From this, it is concluded that unseeded flat flames are virtually insensitive to an electric field because the ion densities at low fuel-air ratios are too low.

The Powling-type burner used in these experiments produces flat flames over a very narrow range of low gas velocities (hence low flame speeds) and fuel-air ratios. Consequently, it was impossible to produce a flat flame with the large ion densities that occur at near stoichiometric fuel-air ratios and large flame speeds. In order to increase the ion densities at the inescapable low velocities and lean mixtures of the Powling-type burner, an alternate procedure of seeding the flame with $\text{KOH} \cdot \text{H}_2\text{O}$ mist was undertaken. While the K^+ ions are unlike combustion ions, valid results are expected because these ions do not alter the chemistry of combustion and the field-flame interaction under study is of mechanical origin.

An order of magnitude analysis revealed that the ion densities for unseeded flat flames were 10^7 to 10^8 ions/cc. Addition of KOH mist to the flame produced a K^+ ion density in the flame of the order 10^{11} ions/cc and negligible amounts at either electrode.

9.3 Seeded Flat Flames

A fine mist of aqueous potassium hydroxide and air was produced by equipment described earlier and was introduced into the fuel and air stream well upstream of the duct exit. The mist had the appearance of cigarette smoke, but no attempt was made to measure droplet size or population. Since the molarity of the aqueous potassium hydroxide

solution was constant throughout all experiments (8.38% KOH mole fraction) it was possible to measure the KOH and water mass flows in the mist. The flow of KOH was found to be 4.77×10^{-3} gm/min. In order to produce a uniform mist, it was necessary to operate at a constant mist flow throughout all experiments. For this reason, low velocity flames contain a slightly higher K^+ density than the higher velocity flames. For the flames studied, the KOH/fuel flow varied over the following range.

$$.51\% < (\text{mass KOH/mass of fuel}) < .67\%$$

Since the amount of KOH added to the flame was small in itself, the above variation of KOH/fuel should have very little influence upon the chemical reactions. One can expect slightly larger ion densities, hence currents at low velocity flames, but even this should be of secondary importance.

The presence of water vapor in the fuel-air stream is of considerable importance and had to be accounted for in all experiments. Water vapor in the unburned gas arose from the inherent humidity of the air, the water vapor acquired by passing the fuel through the wet test meter and that introduced directly by the mist. Of the water vapor present in the unburned mixture, roughly 19% was due to the wet test meter and 15% due to the KOH mist, the remainder arose from the humidity of room air drawn through the centrifugal blower.

A summary of stable seeded flat flames that were obtained with no electric field is shown in Fig. 9-4. While this graph shows only the

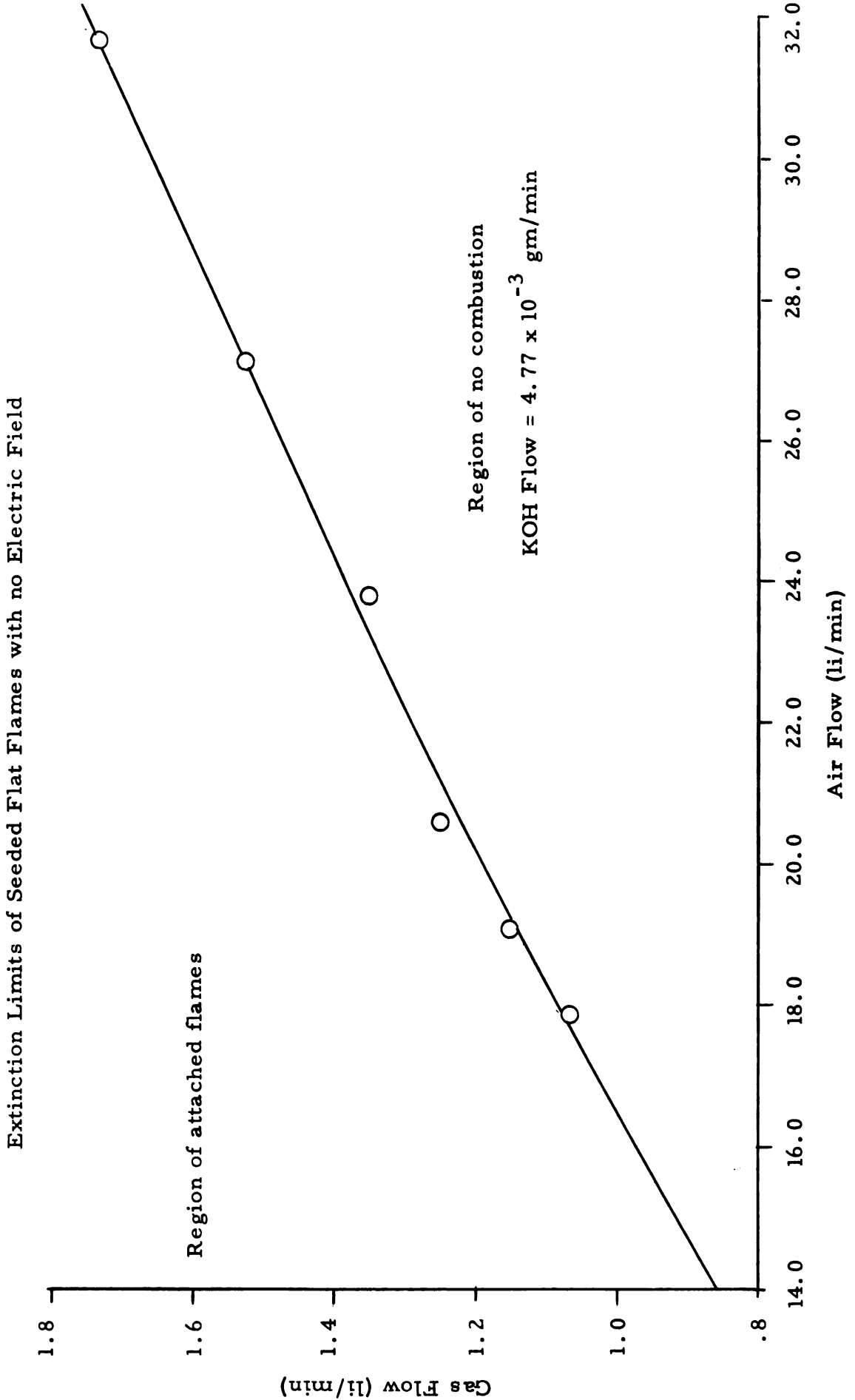


Fig. 9-4

extinction limits, it is to be remembered that stable flat flames lay in a narrow zone adjacent to and just above the curve in Fig. 9-4. Flames occurring at air flows greater than 24 li/min lose a great deal of their flatness and only flames on the lower half of the curve were subjected to electric fields.

For some reason, seeded flat flames displayed shallow cusps or corrugations. The cusps were approximately 1/4" in diameter and 1/16" deep. The basic flatness of the flame was preserved and no attempt was made to analyze these formations. Application of an electric field, positive or negative, destroyed these corrugations and a smooth, steady flame, as shown in Fig. 9-2, was produced.

The cusps encountered in seeded flames are suspected to have an origin similar to those Lewis and Von Elbe⁽⁹⁰⁾ describe for unseeded flames where preferential diffusion and heat transfer coupled with a diverting of the streamlines produce an uneven flame velocity and thus warping of the flame front. What follows is conjecture, but nevertheless stems from accepted theory.

Within the flame vaporization of mist droplets produces temperature gradients and K^+ concentration gradients which are not necessarily in the direction of flow. These local variations in temperature across the flame surface produce higher flame speeds in regions of high temperature which in turn warp the flame sheet into a cusp convex to the unburned flow. The opposite effect is produced in regions of low temperature.

With the application of an electric field, all ions migrate parallel to the direction of flow regardless of any temperature or concentration gradients in other directions. The mechanical effect of the ensuing momentum exchange, then restores the original flatness to the flame.

Cusp formation in unseeded flat flames is not uncommon. Edgerton⁽⁸³⁾ and Dixon-Lewis⁽⁹³⁾ both report the presence of cusps in flat flames of methane and propane.

9.4 Seeded Flat Flames with Positive Electric Fields

When a stable flat flame was produced and a positive electric field (upper grid negative, matrix positive) imposed on the flame, the following sequence of events occurred as the voltage was increased while the air, fuel and mist flows were kept constant.

- (1) (0 - 500 volts) The center portion of the flame was drawn to within 1/8" of the matrix and formed two or three protrusions while the remainder of the flame remained flat.
- (2) (500 - 1000 volts) The outer portions of the flame rose, broke apart and formed unsteady paraboloid - like surfaces with the former protrusions. These flame sheets moved about above the matrix in random fashion.
- (3) (1000 - 2000 volts) The random motion of the flame surfaces decreased, the flame surfaces began to widen at the top and a continuous but undulating flame sheet with a scalloped periphery was formed. The flame was about

1/8" above the matrix and the diameter was roughly equal to the diameter of the duct.

- (4) (above 2000 volts) A continuous and steady flame sheet was formed which displayed a small decrease in diameter as the voltage was increased.

If the voltage changes were reversed, the above sequence was reversed.

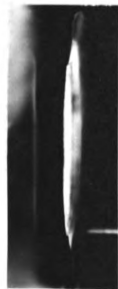
It was observed that for voltages in excess of 2KV, that it was possible to increase the air flow, keeping the gas and mist flows constant, and cause the flame to rise off the matrix. Under these conditions, the flame was a steady continuous disk similar in appearance to the stable flat flames discussed earlier. The blue color of these flames was, however, less intense. The velocity of the gases at the matrix and the fuel-air ratios for these flames was well into the region (Fig. 9-4) where no combustion was possible without an electric field. If the voltage was reduced to zero, the flames were always extinguished.

A series of experiments were conducted in an effort to determine the extent to which a positive electric field widened the lean extinction limits. In these experiments, stable flat flames were produced with no applied voltage; with constant gas and mist flows a fixed voltage was applied across the flame and the air flow increased until extinction occurred. At extinction, gas, air and mist flows were recorded as were the voltage and current.

Appendix B is a summary of data taken. Figures 9-6, 7, 8 show voltage and current readings at extinction for three gas flows



(a) 0 KV, 0 μ A



(b) .14 KV, 1.1 μ A



(c) .4 KV, 4.6 μ A

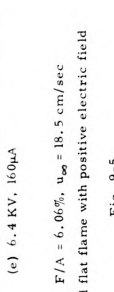
$F/A = 6.06\%$, $u_{99} = 18.5$ cm/sec

Seeded flat flame with positive electric field

Fig. 9-5



(d) .31 KV, 4.6 μ A



(e) 6.4 KV, 160 μ A

Current and Voltage vs Air Flow at Extinction
Positive Electric Field

City Gas Flow = .957 (li/min)
KOH Flow = 4.77×10^{-3} gm/min
d = 3.18cm

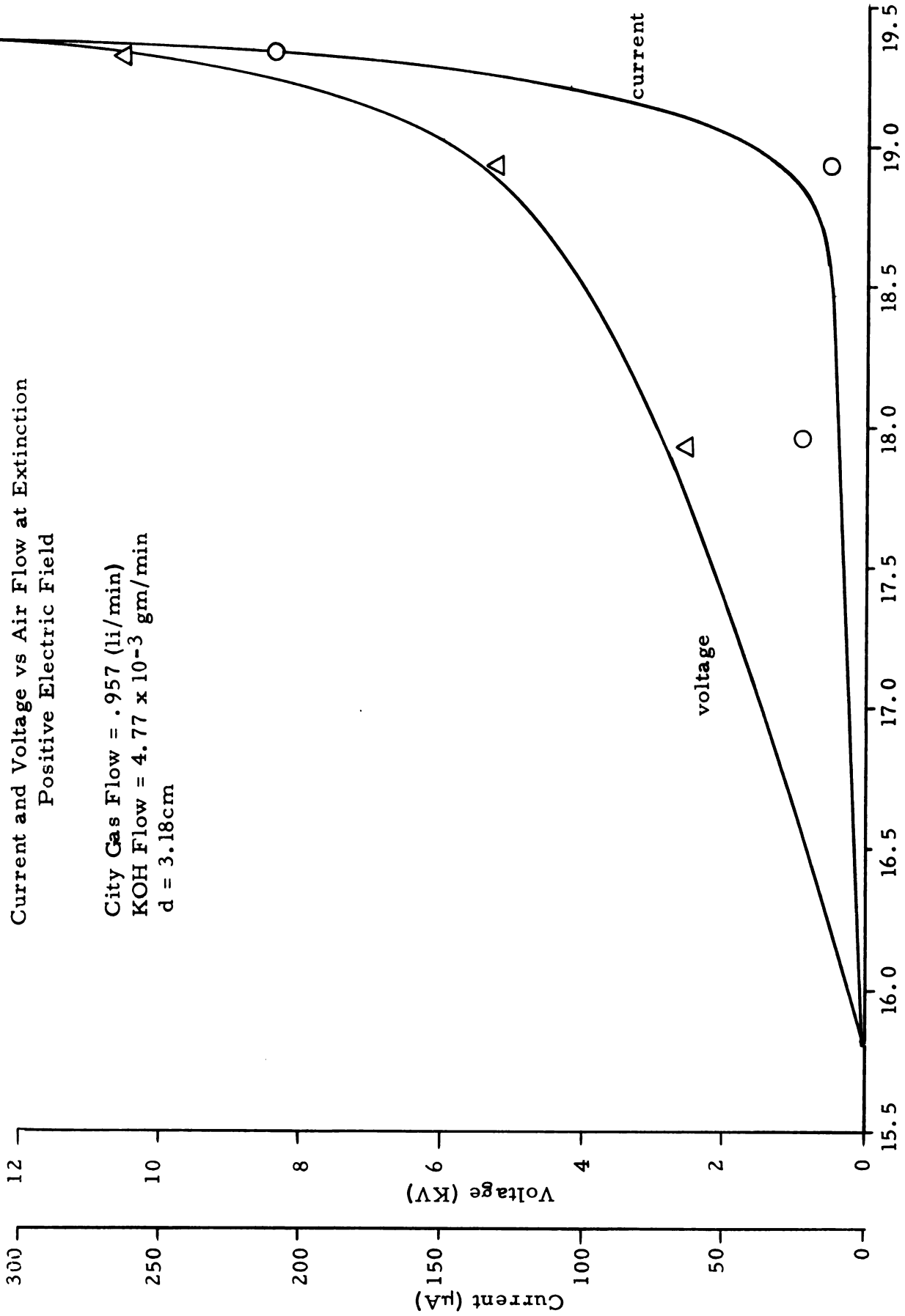


Fig. 9-6

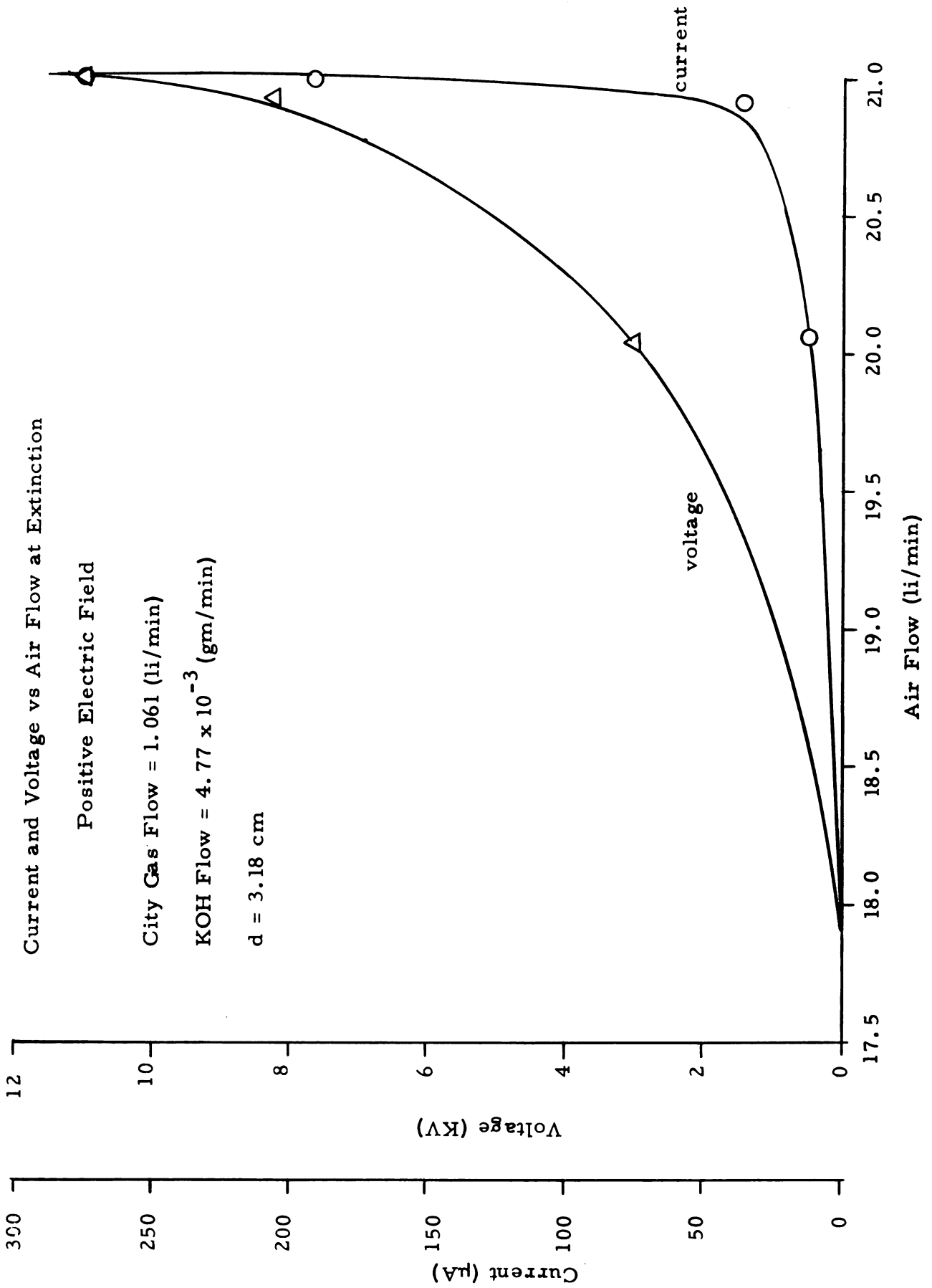
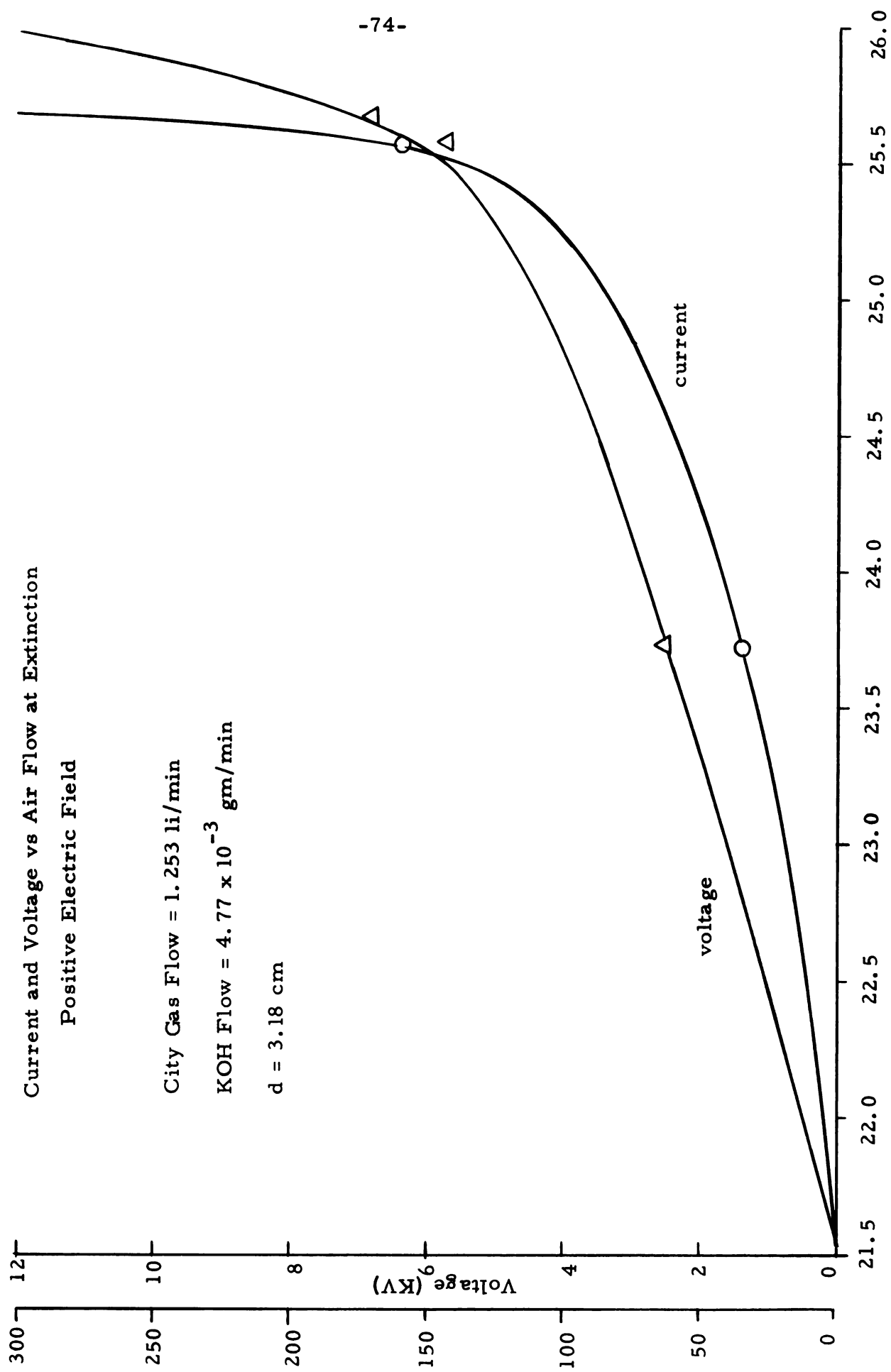


Fig. 9-7



Current and Voltage vs Air Flow at Extinction

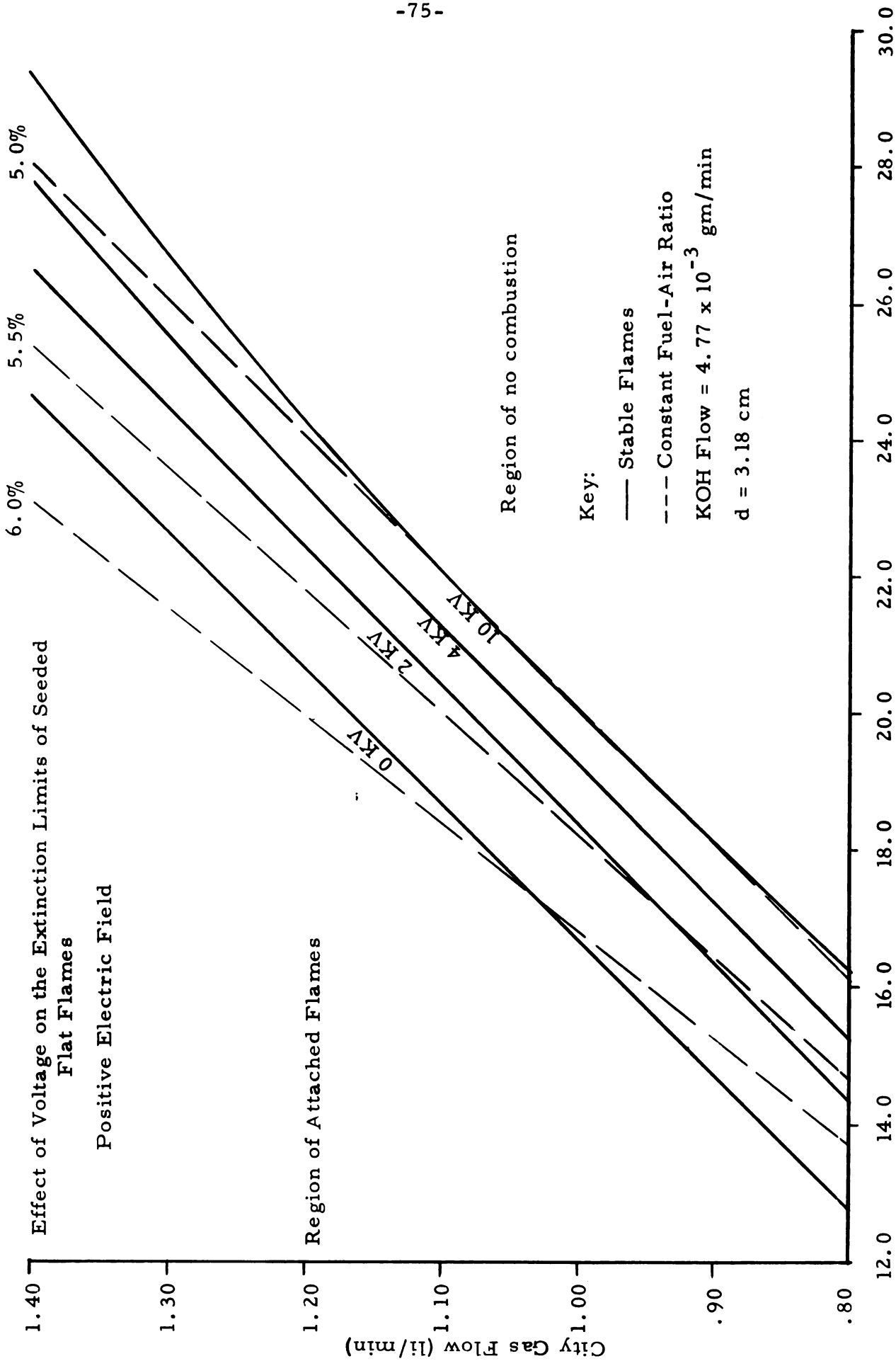
Positive Electric Field

City Gas Flow = 1.253 li/min

KOH Flow = 4.77×10^{-3} gm/min

d = 3.18 cm

Air Flow (li/min)
Fig. 9-8



Air Flow (li/min)

Fig. 9-9

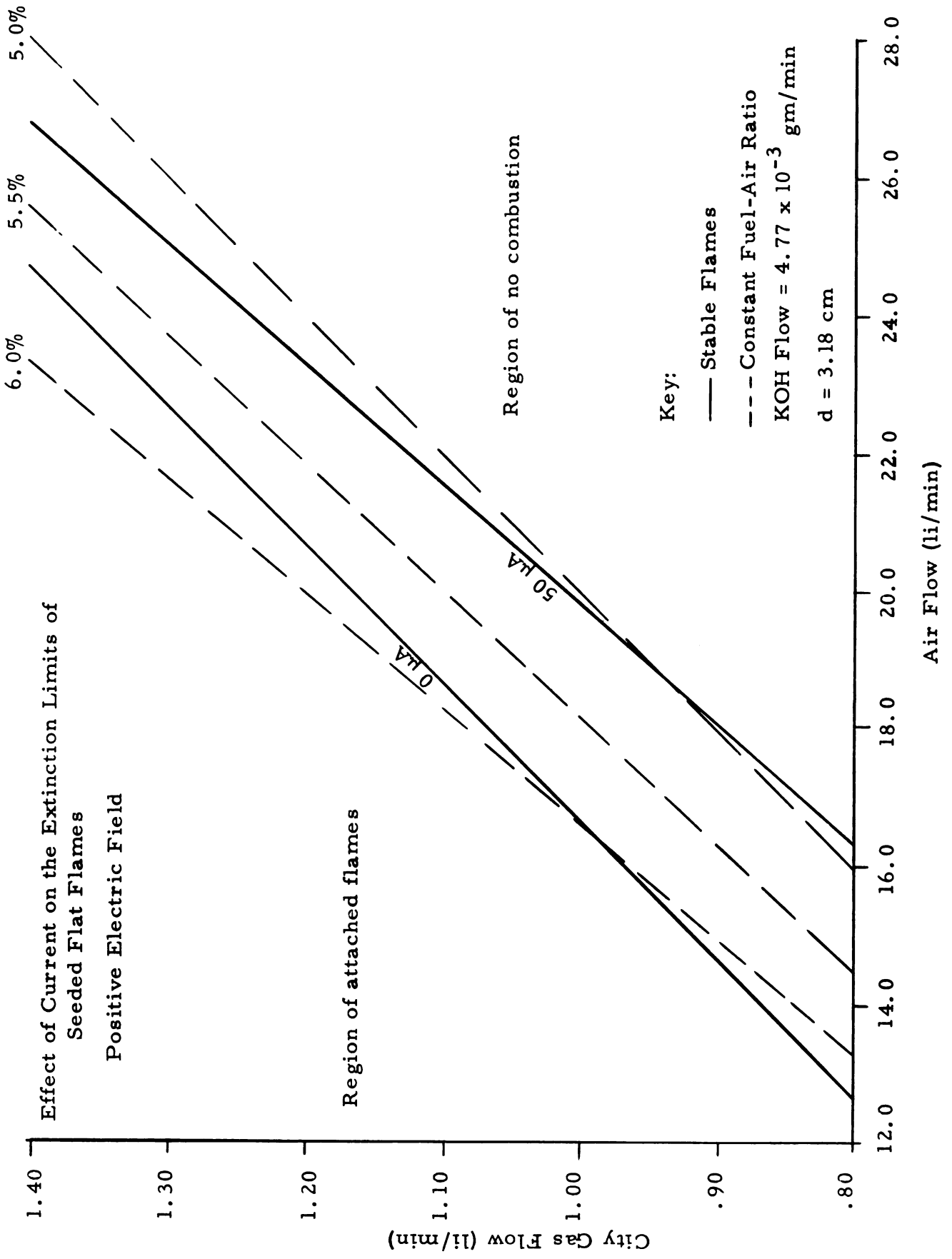


Fig. 9-10

studied. Cross plotting these figures, it was possible to show the widening of the extinction limits as functions of voltage and current.

Figures 9-10, 11 reveal two important effects of positive electric fields.

- (1) At a constant gas flow, positive electric fields allow one to support combustion at progressively higher air flows, hence higher flame velocities since the flame speed is nearly equal to the total gas flow divided by the duct area.
- (2) At a constant air flow, a positive electric field allows one to support combustion at progressively lower fuel flows, hence at lower fuel-air ratios.

9.5 Seeded Flat Flames with Negative Electric Fields

When a stable flat flame was produced and a negative electric field (upper grid positive, matrix negative) imposed on the flame, the following sequence of events occurred as the voltage was increased while the air, fuel and mist flows were kept constant.

- (1) (0 - 250 volts) The center portion of a stable flat flame was drawn down to within 1/8" of the matrix, and a wrinkled flame sheet resembling a "soup bowl" was gradually formed.
- (2) (250 - 1000 volts) The outer portions of the flame were drawn down to the matrix and a slow undulating flame sheet was formed over the matrix. The flame sheet was continuous, but had a scalloped periphery.
- (3) (above 1000 volts) The unsteadiness of the flame disappeared

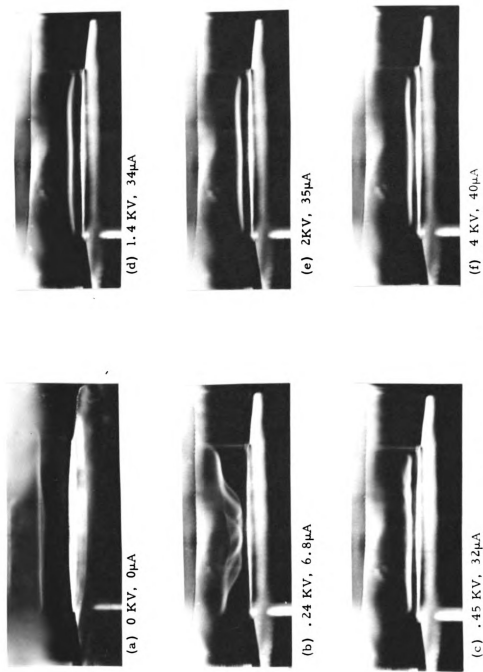
and the flame became a smooth circular disk slightly concave to the flow whose diameter slightly increased as the voltage increased.

Since a positive electric field widened the lean extinction limits, one might expect a negative electric field to narrow the extinction limits. Contrary to such a prediction, experiments revealed that a negative electric field (as the case with a positive field) permitted one to support a flame at fuel-air ratios lower than the lean extinction fuel-air ratio without a field. The experiments described in section 9.4 were repeated for the negative field. Figures 9-12,13 show the results of these experiments.

Comparison of Figs. 9-9, 13 reveals that the relationship between applied voltage and lean extinction has the following differences.

- (1) As the voltage increases, positive fields lower the extinction limits (i. e. permit greater air flow at constant fuel flow) in a more gradual fashion than with negative fields.
- (2) The negative field displays a limiting voltage (approximately 1 KV) above which a further increase in air flow is not possible. Positive fields have no such limit, although above 10 KV only minimal increases in air flow are possible.

In any discussion of the extinction limits of a flame careful attention must be paid to heat sinks, since almost any flame can be sufficiently quenched and combustion stopped. Since the matrix was



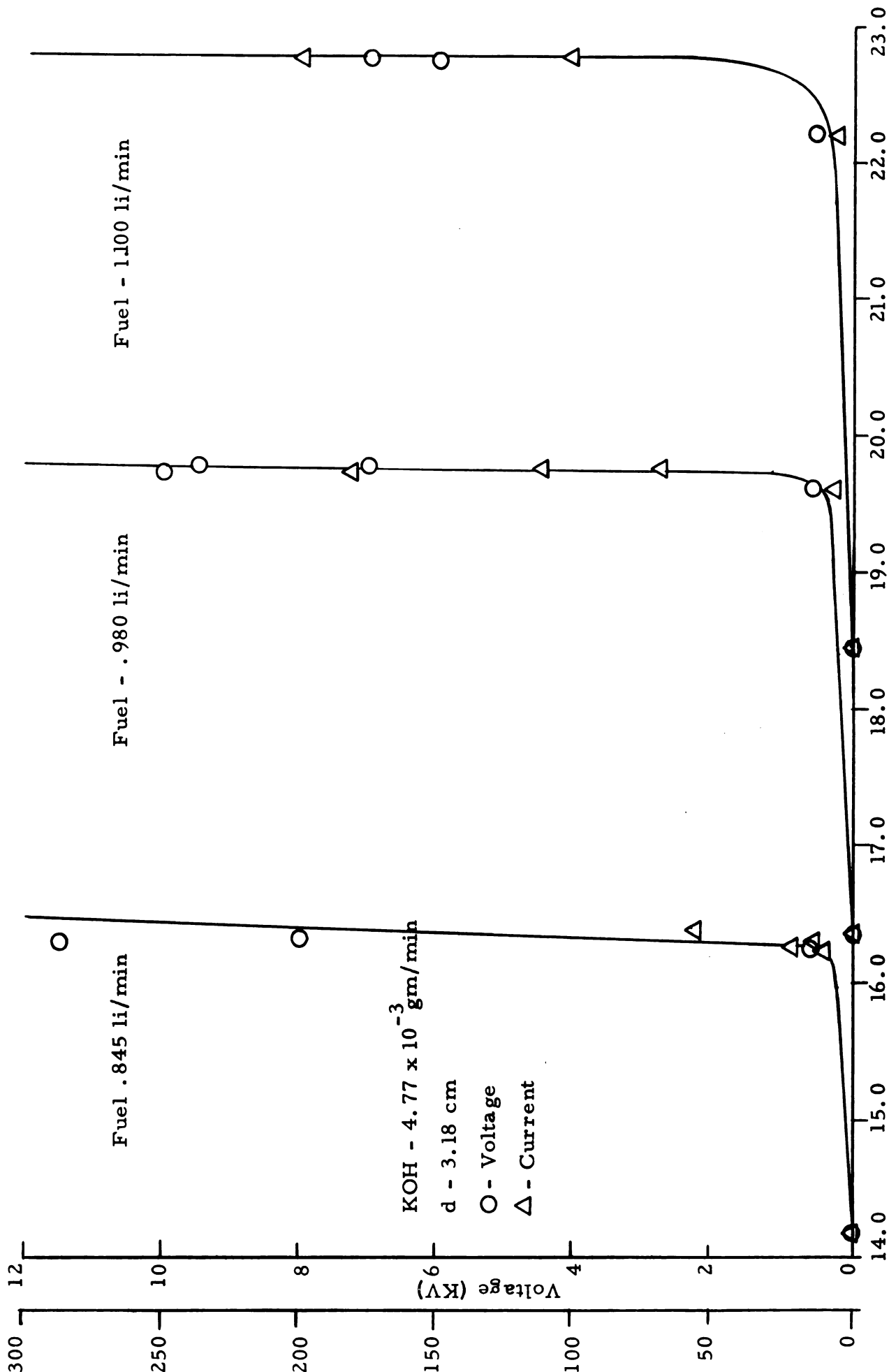
$u_{\infty} = 18.8 \text{ cm/sec}$

$F/A = 6.03\%$

Seeded flat flame with a negative electric field

Fig. 9-11

Effect of Negative Field upon Lean Extinction Limits
Current and Voltage vs Air Flow at Constant
Fuel Flow



Air Flow (li/min)

Fig. 9-12

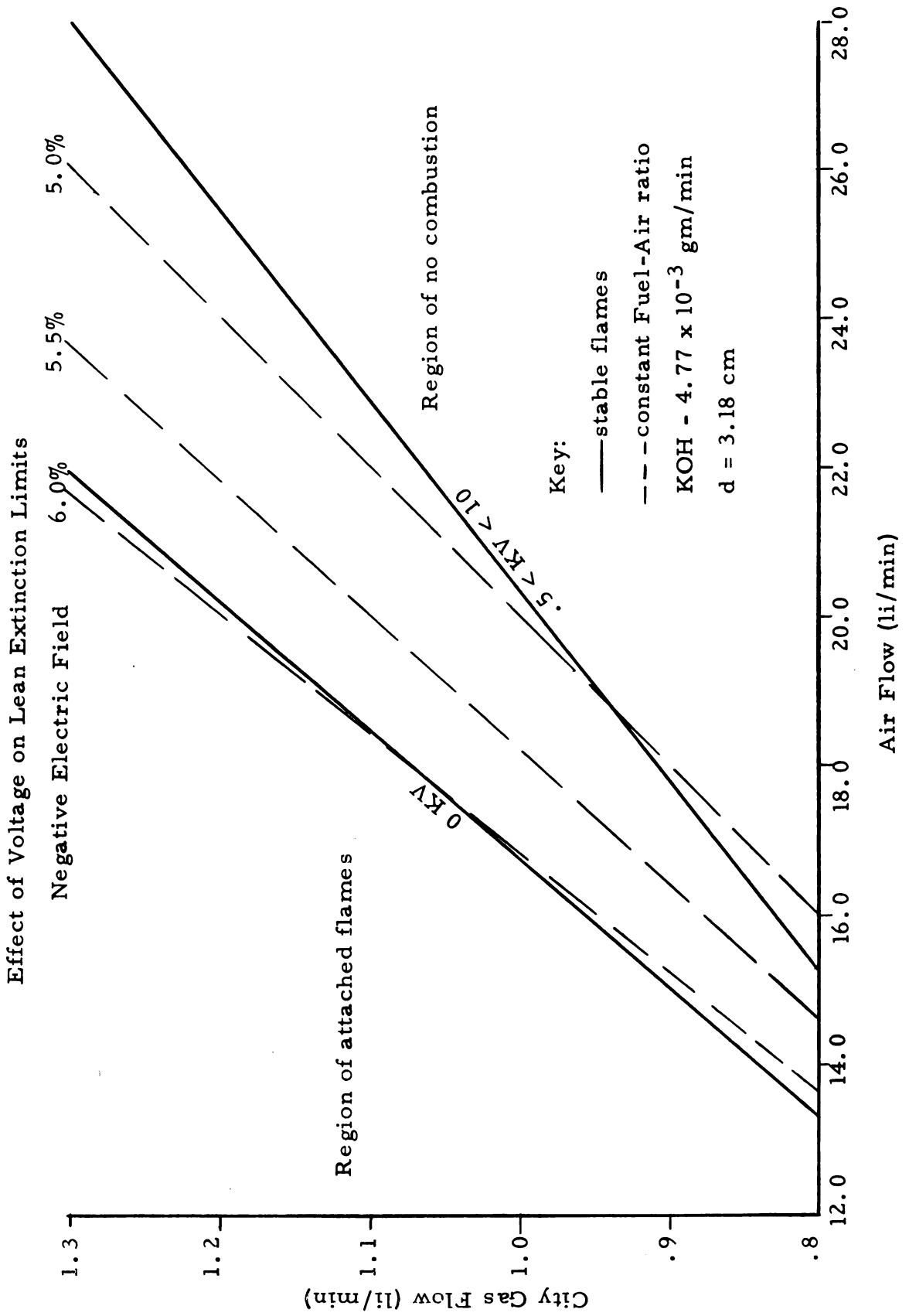
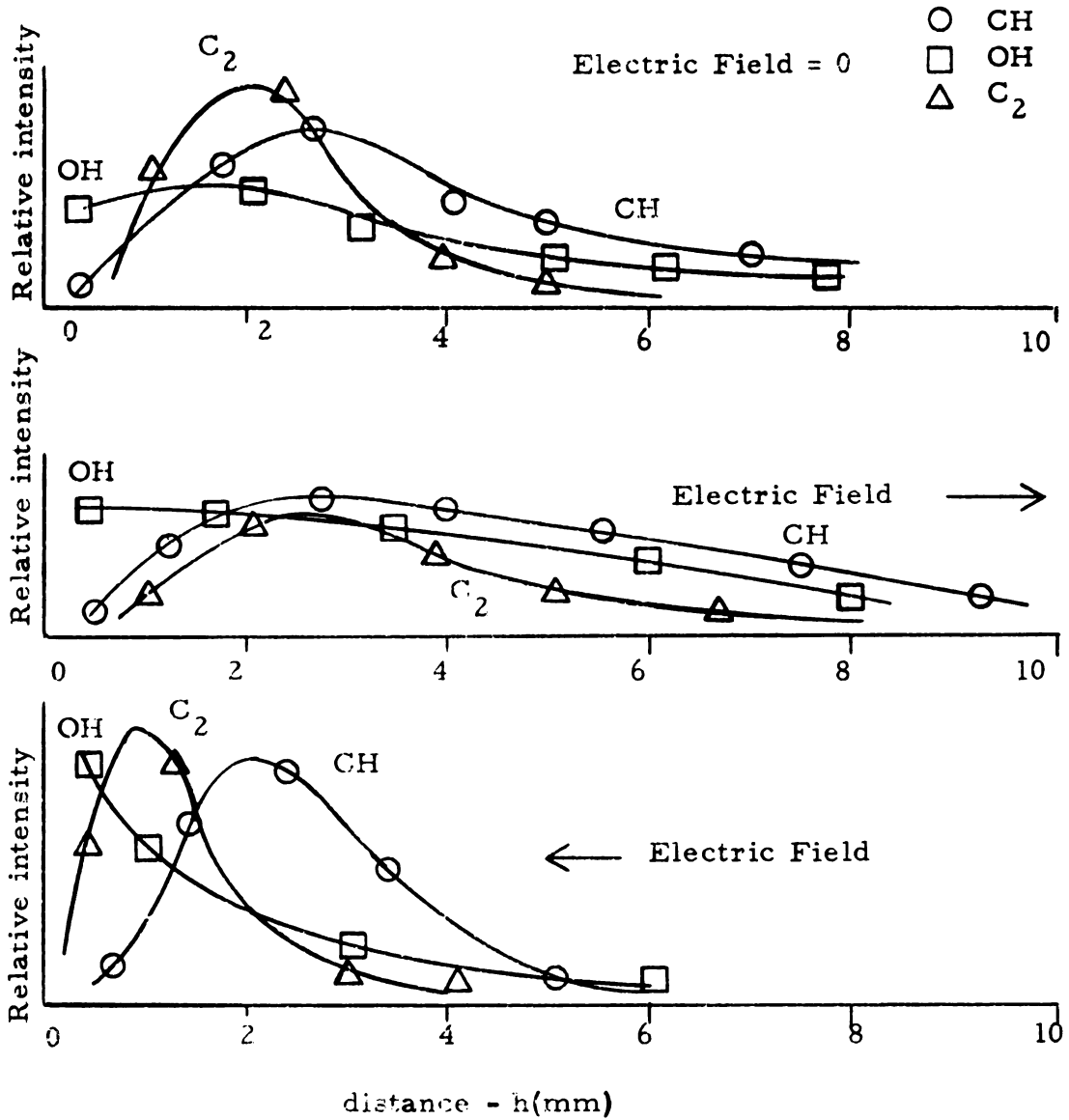


Fig. 9-13

often positive, it was not possible to regulate its temperature with cooling water as Botha and Spalding⁽⁸⁸⁾ had done; nevertheless, extinction occurred when all flames (with and without fields) were midway between matrix and grid. Thus, while the heat absorbed by the matrix was not measured, there is no reason to believe it varied much between experiments or was anything but a constant factor in all experiments. Consequently, extinction of the flames was controlled by heat transfer and diffusion at the flame itself.

A flame may be thought of as a complex chemical reaction which requires a chain reaction of events. In the usual case of a chain reaction, the rate of heat evolution at any point of the system is governed not only by temperature and concentration of reactants, but also by chain-carrier concentration. In a combustion wave chain-carriers are formed at high temperature levels and their concentration at low temperature levels is dependent on diffusion. Since ohmic heating contributes about $1 \text{ cal sec}^{-1} \text{ cc}^{-1}$ to a flame, the influence of an electric field upon the extinction limits is certainly not through this kind of energy input or any temperature increase resulting from it. On the basis of experiment, it has not been determined that electric fields principally influence flames thru an increase in diffusion rather than increases in heat transfer, but such a view is favored in light of experiments by Nakamura. Nakamura⁽⁵⁷⁾ has shown (Fig. 9-14) that the distribution of combustion ions is displaced (in accordance with polarity) by an electric field.



Relative intensity of radical radiation at the base of a propane-air diffusion flame⁽⁵⁷⁾

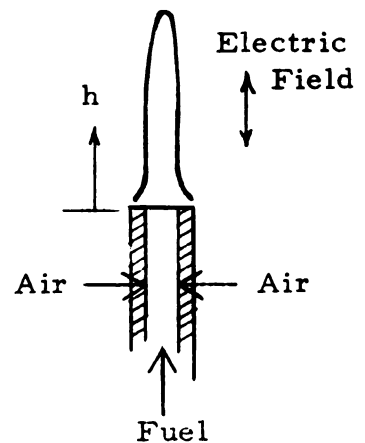


Fig. 9-14

Figures 9-9 thru 13 indicate that both positive and negative ions are essential chain carriers since the lean extinction limits were broadened by fields of both polarity. Negative fields assist positive ions to diffuse into the unburned mixture; thus by increasing the concentration, support chemical reaction that would otherwise not be possible without a field. The converse appears to be true for the case of the positive field. This view is consistent with Gaydon and Wolfhard⁽¹⁶⁾ who contend that for hydrocarbons, the role of diffusion is mainly to trigger the reactions at relatively low temperature and to fix the point where reactions start.

Quantitatively, little else can be concluded from the macroscopic data taken, since the identity and concentration of these essential chain-carriers was not determined.

9.6 Effect of an Electric Field on the Flame Speed

The burning velocities of various flat flames subjected to positive and negative fields were calculated using the following form of

(7-10)

$$S_u = \left(\frac{\text{Duct Area}}{\text{Flame Area}} \right) \text{ Duct Velocity} = \left(\frac{A_d}{A_f} \right) u_d \quad (9-1)$$

A series of experiments (subsections 9.6.1 and 9.6.2) were conducted in which flat flames were studied at constant fuel-air ratio and duct velocity (u_d), but varying positive and negative electric fields. The diameters of the flames were measured visually with a cathetometer (a traveling microscope capable of measuring distances to within .005cm).

As mentioned earlier, any measurement of flame speed using

flat flame burners must carefully consider the effect of quenching in light of the experiments of Botha and Spalding⁽⁸⁸⁾. In these experiments, flat flames were subjected to varying amounts of quenching (controlled cooling of the matrix) and at constant fuel-air ratio it was found that the flame speed decreased linearly with cooling. Typical results is shown in Figure 9-15.

The extrapolated value of flame speed at zero heat flux is referred to as the adiabatic flame speed.

In the experiments of this study, it was not possible to either control or measure the heat extracted from the flame, but sufficient time was always allowed for the establishment of steady state conditions. For each series of experiments, the only variable was the voltage since electrode separation, fuel-air ratio, duct velocity and the vertical position of the flame were constant. Thus, while the measured flame speeds were not the adiabatic values, the effect of heat sinks was a constant factor and all changes in flame diameter were solely attributed to the applied field.

9.6.1 Positive electric fields

At voltages below 2KV, the violent unsteadiness of the flame (section 9.4) prevented any measurement of the flame diameter. Once a flat flame was stabilized at a high voltage, an increase in voltage always produced a reduction in flame diameter. Throughout these changes, the flame lay approximately midway between the electrodes and its vertical position was not observed to change with changes in

Effect of Quenching on the Flame Speed of a Propane-Air
Flame⁽⁸⁸⁾

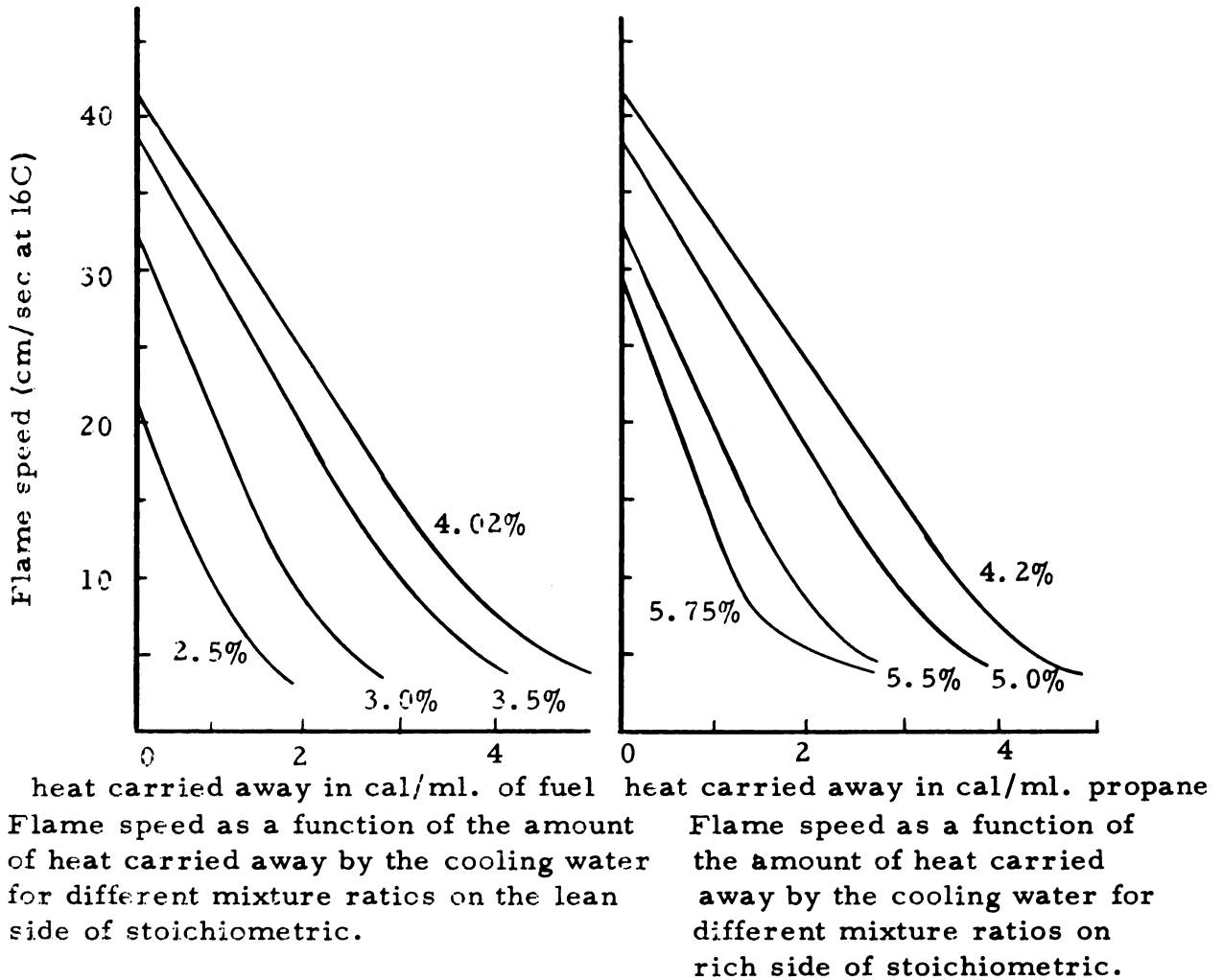


Fig. 9-15

voltage. Over the entire range of applied voltages, the flame diameter varied linearly with the current. Since a reduction of the voltage below a minimal value would cause extinction (see Fig. 9-9), it was not possible to measure the flame size at zero voltage and current. For purposes of comparison, the data was extrapolated to zero current. This flame size was used to calculate S_u^0 . Appendix C, is typical of the data obtained for positive fields.

In order to compare experimental results with the approximate theory of Section 7 (equation 7-22), the following representative properties of city gas were assumed,

- (1) lower heating value (LHV) of city gas = 1021 Btu/ft³ of gas
- (2) $N = N(\text{LHV, fuel-air ratio})$
- (3) $B = 0$
- (4) $T_u = 138^\circ\text{C}$
- (5) $K_+ = \text{mobility of potassium} = 2.7 \text{ cm}^2 \text{ volt}^{-1} \text{ sec}^{-1}$ (47)
- (6) $l = 10^{-2} \text{ cm}$ (46)

Figure 9-16 shows the experimental values of flame speed calculated from (9-1) and also those obtained from (7-22) for two flame thicknesses.

9.6.2. Negative electric fields

The violent unsteadiness experienced by the flame at low positive fields did not occur with negative fields and it was possible to measure variations in flame speed at voltages below 1KV. As the voltage was slowly increased from zero (the fuel-air ratio and duct

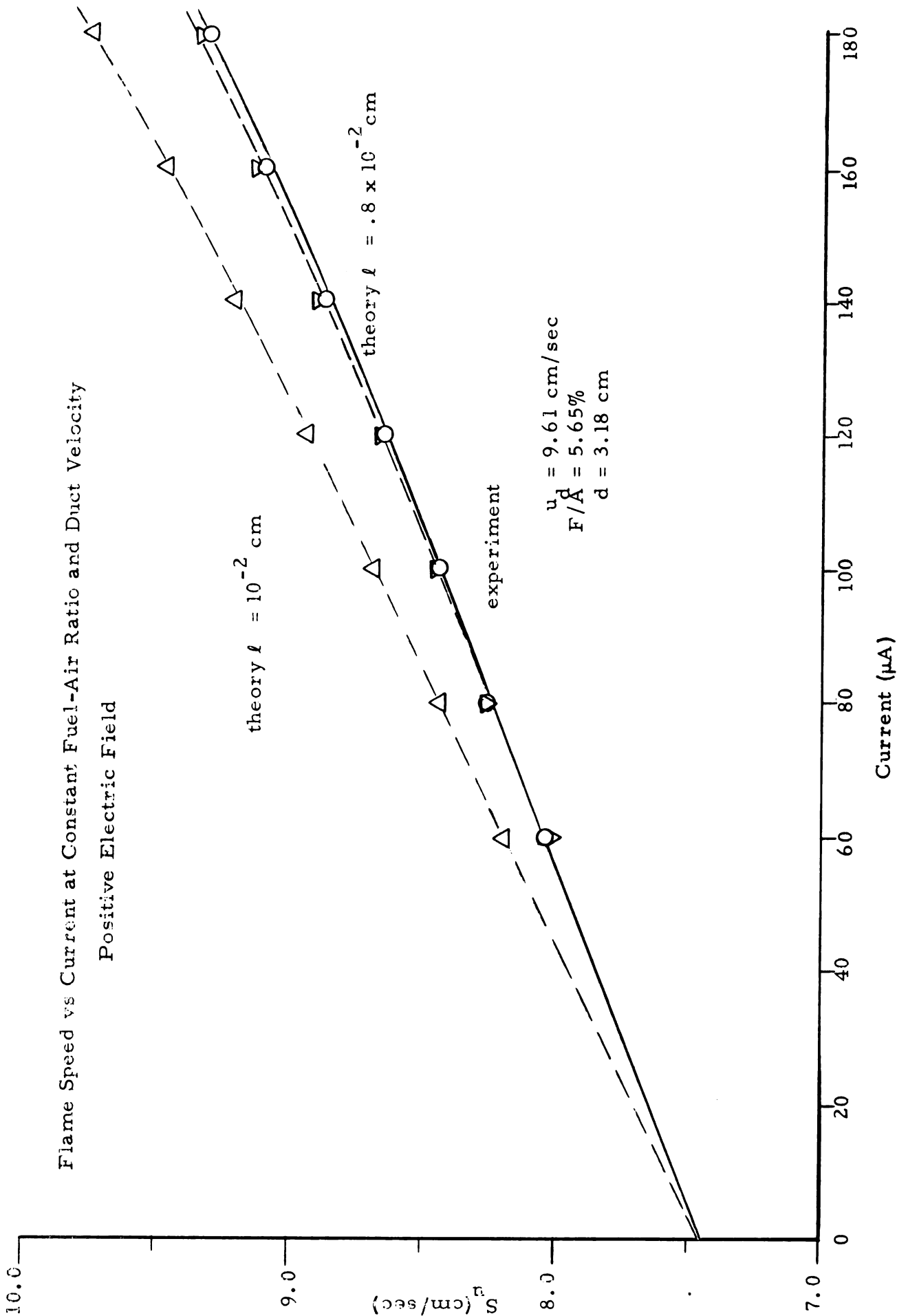


Fig. 9-16

velocity remaining constant) the flame was drawn down to within 1/4" of the matrix. At low voltage (100-200 volts) some unsteadiness and cusps developed, but as the voltage was increased, a thin, steady flame sheet with a small peripheral lip was produced. As the voltage increased, the flame diameter increased, the increase being linear with respect to the measured current. Throughout these changes, the vertical position of the flame did not change. As before, the flame speed at zero current and field was that calculated from (9-1) using the flame diameter extrapolated from the experimental measurements. Appendix C, is typical of the data obtained for negative fields. Figure 9-17 shows the experimental values of flame speed and also those values of the flame speed obtained from (7-22) and the previous representative properties of city gas.

Figures 9-16 and 17 show that experimental results agree favorably with approximate theory. The linearity between flame speed and current is clear in all the curves, but the choice of a value of l , the flame thickness, is quite important if complete agreement is to be obtained. The length l is taken to be the thickness of the luminous region of the flame since it is within this region that the ion densities reach significant proportions.⁽⁴³⁾ Since the species concentrations have smooth distributions and the luminous region does not have distinct edges, some flexibility in choosing l is to be expected. The different values of l used to obtain complete confirmation of theory and experiment are well within the experimental accuracy to measure the flame thickness.

Flame Speed vs Current at Constant Fuel-Air
Ratio and Duct Velocity
Negative Electric Field

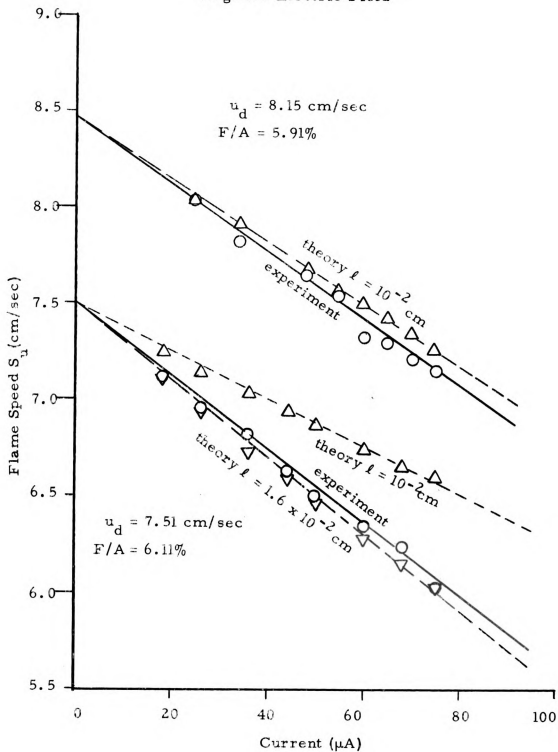


Fig. 9-17

10. CONCLUSIONS

As a result of the analyses and experiments conducted, the following conclusions are made.

1. For combustion processes where the kinetic mechanisms are known and where;

(a) the binary diffusion coefficients are related through an overall diffusion coefficient ρ ,

(b) the heat transfer by thermal conduction and diffusion balance,

(c) the longitudinal electric and transverse magnetic fields are constant,

a method of successive approximations is proposed whereby the equations of combustion can be solved. Solution of these equations yields the species and temperature profiles from hot to cold boundary, and the flame speed.

2. By considering a flame as a layer of ions of finite thickness, it is possible to predict the burning velocity of a flame under the influence of a uniform longitudinal electric field and transverse magnetic field. Such an equation is based on the notion of the Chattock electric wind and requires only a knowledge of the current through the flame, positive ion mobility, and usual combustion variables. Use of this equation yields results which agree favorably with experiment.

3. Experiments reveal that electric fields enable one to support a flat flame seeded with KOH mist at lean fuel-air ratios

where extinction would occur were no field present. Such improvement is possible with electric fields of both polarity.

BIBLIOGRAPHY

1. von Karman, T. and Millan, G., "Thermal Theory of a Laminar Flame Front Near a Cold Wall," Fourth Symposium on Combustion, Baltimore: Williams and Wilkins Co., 1952, pp.173-7.
2. Hirschfelder, J.O., Curtiss, C.F., Campbell, D.E., "The Theory of Flames and Detonations," Fourth Symposium on Combustion, Baltimore: Williams and Wilkins Co., 1952, pp. 190-211.
3. Hirschfelder, J.O., Curtiss, C.F., Bird, R.B., "Molecular Theory of Gases and Liquids," New York: Wiley and Sons, Inc., 1954.
4. Emmons, H.W. (Editor), "Fundamentals of Gas Dynamics," Volume III High Speed Aerodynamics and Jet Propulsion, Princeton: Princeton University Press, 1958, pp. 574-686.
5. Bird, R. B., Stewart, W. E., Lightfoot, E.N., "Transport Phenomena," New York: John Wiley and Sons, 1960.
6. Grad, H., "Notes on Magneto-Hydrodynamics - Number I," Report, AEC Computing Facility, Institute of Mathematical Sciences, New York University, August 1956.
7. Chapman, S., Cowling, T.G., "The Mathematical Theory of Non-Uniform Gases," London: Cambridge University Press, 1960.
8. Beck, J. V., "MHD Effects Upon Laminar Flame Propagation," AVCO Report, work order G258-21F-4478, Dept. T435 act 1960.
9. Hirschfelder, J.O., "Theory of Flames Produced by Unimolecular Reactions," Part I and II, American Institute of Physics, The Physics of Fluids, Vol. 2, No. 5, Sept-Oct. 1959, pp. 551-74.
10. Chu, Boa-Teh, "Thermodynamics of Electrically Conducting Fluids," American Institute of Physics, The Physics of Fluids, Vol. 2, No. 5, Sept. -Oct. 1959, pp. 473-84.
11. Calcote, H.F., Pease, R.N., "Electrical Properties of Flames," Industrial and Engineering Chemistry, Dec. 1951, pp. 2726-2731.
12. Calcote, H.F., "Electrical Properties of Flames," Third Symposium on Combustion, Flame and Explosion Phenomena," Baltimore: Williams and Wilkins Co., 1949, pp. 245-53.

13. Rosnow, V. J., "On Flow of Electrically Conducting Fluids Over a Flat Plate in the Presence of a Transverse Magnetic Field," NACA Report 1358, n. d.
14. Fano, R. N., Chu, L. J., Adler, R. B., "Electromagnetic Fields, Energy, and Forces," New York: John Wiley and Sons, 1960.
15. Lewis, B., "The Effect of an Electric Field on Flames and Their Propagation," Journal American Chemical Society, Vol. 53, pp. 1304-1313, 1931.
16. Gaydon, A. G., Walfhard, H. G., "Flames, Their Structure Radiation and Temperature," London: Chapman and Hall, Ltd., 1961.
17. Penner, S. S., "Introduction to the Study of Chemical Reactions in Flow Systems," Advisory Group for Aeronautical Research and Development NATO, London: Butterworths Scientific Publications, 1955.
18. Thomson, J. J., Thomson, G. P., "Conduction of Electricity Through Gases," Vol. I, Third Edition, 1928.
19. Wilson, H. A., "The Electrical Properties of Flames and of Incandescent Solids," London University Press, 1912.
20. Wiedermann, "Elektricität," Vol. 4B, Chp. 4, 1895.
21. de Hemptinne, "Z. Physik. Chem." 12, pp. 244-74, 1893.
22. Faraday, M., "Experimental Research in Electricity," Quaritch, London, vol. 1, 1839.
23. Lind, S. C., "Miscellaneous Notes on Gas Kinetics," Journal of Physical Chemistry, vol. 28, pp. 57, 1924.
24. Malinowsky, Journal Chem. phys., Vol. 21, pp. 469, 1924.
25. Malinowsky and Lawrow, Z. Physik, Vol. 59, pp. 690, 1930.
26. Mukherjee, N., "Ionization Mechanism and Ion Population in Flames," paper no. 2584-62, New York: American Rocket Society Ions in Flames and Rocket Exhausts Conference, Oct. 1962.
27. Thorton, Phi. Mag., Vol. 9, pp. 260, 1930.

28. Guenault, E.N., and Wheeler, R.V., "Propagation of Flame in Electric Fields," Part I and II, J. Chem. Society, Vol. 134, pp. 195, 1931, Vol. 135, p. 2788, 1932.
29. Wendt, G.L., Grimm, F.V., "A Suggested Mechanism for Antiknock Action," Ind. Eng. Chem, Vol. 16, No. 9, pp. 890, 1924.
30. Garner, W.E., and Saunders, S.W., Trans. Faraday Soc., Vol. 22, pp. 281-324, 1926.
31. Franklin J., Munson, M., Field, F., "Chemi-Ionization and Ion-Molecule Reactions in Gases," paper no. 2579-62, New York: American Rocket Society Ions in Flames and Rocket Exhausts Conference, Oct. 1962,
32. Marx, E., Ann. der Physik, Band 2, 1900.
33. Dixon, H.B., Campbell, C., Slater, W., "Photographic Analysis of Explosions in the Magnetic Field," Roy. Soc. of London, Proceedings, Vol. 90, 1914.
34. Bone, W.A., Fraser, R. P., Wheeler, W.H., "Flame Propagation in an Electric Field," Proceedings of the Royal Society Ser. A, Vol. 132-133, pp. 1, 1931.
35. Klein, G., "Contribution to Flame Theory," Phil. Trans. Roy. Soc. London, Ser. A., No. 967, Vol 249, pp. 389, 1957.
36. Asakawa, Y., "Physical Methods for Improving Combustion," Sixth Symposium on Combustion, New York: Reinhold Corp., pp. 923.
37. Beck, J.V. Toong, T.Y., "Magnetogasdynamics Effects on Laminar Flame Propagation," Journal of the Aerospace Sciences, Nov. 1961, Vol. 28, No. 11, pp. 908.
38. von Karman, T., Penner, S.S., "Fundamental Approach to Laminar Flame Propagation," Selected Combustion Problems, AGARD, London: Butterworths Scientific Publications, 1954, pp. 5-41.
39. Campbell, E.S., Hirschfelder, J.O., Schalit, L.M., "Deviation from the Kinetic Steady-State Approximation in a Free-Radical Flame," Seventh Symposium on Combustion, London: Butterworths Publications, 1959, pp. 332.

40. Giddings, J.C., Hirschfelder, J.O., "Flame Properties and the Kinetics of Chain-Branching Reactions," Sixth Symposium on Combustion, New York: Reinhold, 1957, pp. 199.
41. Poncelet, J., Berendsen, R., Van Tiggelen, A., "Comparative Study of Ionization in Acetylene - oxygen and Acetylene -Nitrous Oxide Flames," Seventh Symposium on Combustion, London: Butterworths Scientific Publishers, pp. 256, 1959.
42. Deckers, J., Van Tiggelen, A., "Ion Identification in Flames," Seventh Symposium on Combustion, London: Butterworths Scientific Publishers, pp. 254, 1959.
43. Calcote, H.F., King, I.R., "Studies of Ionization in Flames by Means of Langmuir Probes," Fifth Symposium on Combustion, New York: Reinhold, pp. 423, 1955.
44. Sugden, T.M., "Microwave Studies in the Ionization of Alkali Metals in Flame Gases and Related Phenomena," Fifth Symposium on Combustion, New York: Reinhold, pp. 406, 1955.
45. Bone, W.A., Townend, D. T.A., "Flame and Combustion in Gases," Longmans and Green, London, 1927.
46. Jost, W., "Explosion and Combustion Processes in Gases," New York: McGraw Hill, 1946.
47. Loeb, L.B., "Basic Processes of Gaseous Electronics," Univ. of Calif. Press, 1955.
48. Glockler, G., Lind, S.C., "The Electrochemistry of Gases and other Dielectrics," New York: Wiley and Sons, 1939.
49. Saha, M.N., "Ionization in the Solar Chromosphere," Philosophical Magazine and Journal of Science, Vol. 40, pp. 472, 1920.
50. Inozemtsev, N.N., "Ionization in Laminar Flames," ARS Journal, Vol. 32, No. 7, pp. 1130, July 1962.
51. Curtiss, C.F., Hirschfelder, J.O., Taylor, M., "Propagation of $A \rightleftharpoons B \rightarrow C$ Flames," American Institute of Physics, The Physics of Fluids, Vol. 4. No. 6, pp. 771, June 1961.
52. Polovin, R.V., Demutskii, V.P., "Magnetohydrodynamic combustion," Soviet Physics JETP, Vol. 13, No. 6, pp. 1229-1234, Dec. 1961, (Translation of Zh. Eksp. Teor. Fiz., USSR 40, 1746-1754, June 1961, by Amer. Inst. of Physics Inc.).

53. Payne, K.G., Weinberg, F.J., "Field-induced Ion Movements in Flames," Proc. Roy. Soc. London, Vol. A250, pp. 316-336, 1959.
54. Ward, F.J., Weinberg, F.J., "Photographic Recording of Slow Ions from Flames," Eighth Sym. on Combustion, Baltimore: Williams and Wilkins, pp. 217-22, 1962.
55. Payne, K.G., Weinberg, F.J., "Measurements on Field-induced Ion Flows from Plane Flames," Eighth Symposium on Combustion, Baltimore: Williams and Wilkins, pp. 207-16, 1962.
56. Van Tiggelen, A., "Ionization Phenomena in Flames," paper no. 2582-62, American Rocket Society Ions in Flames and Rocket Exhausts Conference, Oct. 1962.
57. Nakamura, J. "Effect of the Electric Field upon the Spectra of the Hydrocarbon Diffusion Flames," Combustion and Flame, vol. 3, pp. 277, 1957.
58. Kinbara, T., Ikegami, H., "On the Positive and Negative Ions in Diffusion Flames," Combustion and Flame, Vol. 1, pp. 199, 1957.
59. Deckers, J., van Tiggelen, A., "Extraction of Ions from a Flame," Combustion and Flame, vol. 1, pp. 281, 1957.
60. Calcote, H.F., "Mechanisms for the Formation of Ions in Flames," Combustion and Flame, Vol. 1, 1957, pp. 385.
61. Calcote, H.F., "Ion Production and Recombination in Flames," Eighth Symposium on Combustion, Baltimore: Williams and Wilkins, pp. 184-199, 1962.
62. Fueno, T., Mukherjee, N.R., Ree, T., Eyring, H., "Mechanism of Ion Formation in High-Temperature Flames," Eighth Symposium on Combustion, Baltimore: Williams and Wilkins, pp. 222-30, 1962.
63. Richardson, D.L., Karlovitz, B., "A Burner with an Electrical Discharge Superimposed on the Combustion Flame," ASME paper 61 WA251, Dec. 1961.
64. DeJaegere, S., Deckers, J., Van Tiggelen, A., "Identity of the Most Abundant Ions in some Flames," Eighth Combustion Symposium, Baltimore: Williams and Wilkins, pp. 155-60, 1962.

65. Mukherjee, N.R., Fueno, T., Eyring, H., Ree, T., "Ions in Flames," Eighth Symposium on Combustion, Baltimore: Williams and Wilkins, 1962, pp. 1-22.
66. Knewstubb, P.F., Sudgen, T.M., "Mass Spectrometry of the Ions Present in Hydrocarbon Flames," Seventh Symposium on Combustion, London: Butterworths Scientific Publishers, pp. 247, 1959.
67. Wilson, H.A., "Electrical Conductivity of Flames," Review of Modern Physics, Vol. 3, pp. 156, 1931.
68. Calcote, H.F., "Ion and Electron Profiles in Flames," Ninth Symposium on Combustion, New York: Academic Press (in print).
69. Green, J.A., Sugden, T.M., "Some Observations on the Mechanism of Ionization in Flames Containing Hydrocarbons," Ninth Symposium on Combustion, New York: Academic Press, (in print).
70. Adler, J., Spalding, D.B., "Flame Propagation by Non-branching Chain Reactions," Combustion and Flame, Vol. 5, pp. 123, 1961.
71. Spalding, D.B., "Predicting the Laminar Flame Speed in Gases with Temperature - explicit Reaction Rates," Combustion and Flame, Vol. 1, pp. 287, 1957.
72. Spalding, D.B., "One-dimensional Laminar Flame Theory for Temperature-explicit Reaction Rates," Combustion and Flame, Vol. 1, pp. 296, 1957.
73. Adler, J., "The Limits of the Eigenvalue of the Laminar Flame Equation in Terms of the Reaction Rate - Temperature Centroid," Combustion and Flame, Vol. 3, pp. 389, 1959.
74. Klein, G., "Equations of a Simple Flame Solved by Successive Approximations to the Solution of an Integral Equation," Part I, II, III, IV, V, ONR, Univ. of Wisconsin.
75. Klein, G., "Derivation of the Flame Equations, Their Transformation, and a Suggested Method of Their Solution," ONR Univ. of Wisconsin, 1955.
76. Stratton, J.A., "Electromagnetic Theory," New York: McGraw-Hill, 1941.

77. Fano, R., Chu, L., Adler, R., "Electromagnetic Fields, Energy and Forces," New York: John Wiley and Sons, 1960.
78. von Karman, T., "Fundamental Equations in Aerothermochemistry," Selected Combustion Problems II, AGARD, London: Butterworths Scientific Publications, 167-184, 1956.
79. Hirschfelder, J.O., "Diffusion Coefficients in Flames and Detonations with Constant Enthalpy," American Institute of Physics, Physics of Fluids, Vol. 3, pp. 109, 1960.
80. Weinberg, F.J., "Future Research and Unsolved Problems, Combustion and Flame, Vol. 6, No. 1, pp. 59, 1962.
81. Friedman, R., "Measurement of the Temperature Profile in a Laminar Flame," Fourth Symposium on Combustion, Baltimore: Williams and Wilkins, pp. 259, 1953.
82. Powling, J., "The Flat Flame Burner," Experimental Methods in Combustion Research, AGARD Manual, Pergamon Press pp. 1961, Section 2.2.1, pp. 14.
83. Egerton, A., Thabet, S.K., "Flame Propagation: The Measurement of Burning velocities of Slow Flames and the Determination of Limits of Combustion," Proc. Roy. Soc. A211, pp. 445, 1952.
84. Moore, G.E., "Experimental Studies of Some Electrical Properties of Seeded Flame Gases," ARS paper no. 2590-62, Ions in Flames and Rocket Exhausts Conference, Oct.10-12, 1962.
85. "Engineering Aspects of Magnetohydrodynamics," Columbia Univ. Press, 1962.
86. Levy, A., Weinberg, F.J., "Conclusions Concerning Propagation of Flat Flames," Seventh Symposium on Combustion, Butterworths Scientific Publications, London, 1959, pp. 296-303.
87. Helliwell, J.B., "Gas-ionizing Shock and Combustion Waves in Magnetogasdynamics," Journal of Fluid Mechanics, Cambridge University Press, Vol. 14, Part 3, pp. 405-419, 1962.

88. Botha, J.P., Spalding, D.B., 'The Laminar Flame Speed of Propane/Air Mixtures with Heat Extraction From the Flame,' Proceedings of the Royal Society of London A 225, pp. 71, 1954.
89. Mullins, B.P., Penner, S.S., "Explosions, Detonations, Flammability and Ignition," Pergamon Press, New York, 1959.
90. Lewis, B., von Elbe, G., "Combustion, Flames and Explosions of Gases," Second Edition, Academic Press, New York, 1961.
91. Spalding, D.B., "The Theory of Flame Phenomena with a Chain Reaction," Transactions Royal Society of London, A249, pp. 1, 1957.
92. De Sendagorta, J.M., "Propagation Velocity and Structure of Single Step Reaction Flames," Combustion and Flame, Vol. 5, pp. 305, 1961.
93. Dixon-Lewis, G., Isles, G.L., "Flames in Mixtures of Methane and Air Near the Lower Limit of Flammability," Transactions, Faraday Society, vol. 53, part 1, pp. 193, 1957.
94. Minkoff, G.J., Tipper, C.F.H., "Chemistry of Combustion Reactions," London: Butterworths, 1962.

Appendix A
Equipment

1. Burke and James 4" x 5" View Camera, Tessar 1:4.5, f = 21cm lens.
2. "Precision" Wet Test Meter, .1 ft³ per rev, .001 ft³ smallest division, Precision Scientific, Co., Chicago, Ill.
3. American Meter Co., 1 ft³ per rev, .01 ft³ smallest division, American Meter Co., N. Y., N. Y.
4. Standard Timer, .01 min per rev, .001 min smallest division, Standard Electric Time Co., Springfield, Mass.
5. Centrifugal Blower, Buffalo Forge Co., Buffalo, N. Y.
6. Model 500-BB Nobatron Power Supply, 600V DC output, Sorensen and Co., Stanford, Conn.
7. High-Voltage power supply, 75KV DC, 2.5 milliamp, Takk Corp., Neward, Ohio.
8. Model 410B VTVM, Model 459A DC Multiplier, Hewlett Packard, Palo Alto, Calif.
9. Model 210 Electrometer, Model 2008 decade shunt, range 10⁻³ to 10⁻¹² amps, Keithley Instruments, Cleveland, Ohio.
10. Cathetometer, W. G. Pye and Co. Ltd., Cambridge, England.

Appendix B
Data Extinction Limits of Seeded Flat Flames

Positive Electric Field				Negative Electric Field			
Fuel li/min	Air li/min	KV	μ A	Fuel li/min	Air li/min	KV	μ A
.957	15.672	0	0	.844	14.157	0	0
.957	17.951	2.5	22	.845	16.247	.5	8
.957	18.942	5.2	10	.845	16.307	8.0	12
.957	19.368	10.5	210	.844	16.277	11.5	20
				.853	16.534	15.0	55
1.069	17.931	0	0	.980	16.327	0	0
1.063	20.061	3.0	12	.973	19.616	.5	5
1.069	20.933	8.2	34	.982	19.764	7.0	68
1.066	21.012	11	190	.982	19.764	9.5	110
				.975	19.705	10.0	180
1.251	21.577	0	0	1.099	18.427	0	0
1.257	23.727	2.5	34	1.101	22.191	.5	1
1.254	25.579	5.7	158	1.101	22.736	6	100
1.269	25.678	6.8	340	1.099	22.766	7	200

KOH flow = 4.77×10^{-3} gm/min

electrode separation = 3.18 cm

Appendix C

Data-Effect of Electric Field Upon Flame Speed

Positive Field			Negative Fields		
Fuel = 1.004 li/min Air = 17.775 li/min			Fuel = .846 li/min Air = 13.833 li/min		
μA	KV	$D_f(\text{cm})$	μA	V	$D_f(\text{cm})$
60	4.60	8.33	18	200	7.805
70	4.70	8.29	26	250	7.915
80	4.80	8.22	36	300	7.995
90	4.88	8.19	44	350	8.115
100	4.95	8.13	50	400	8.195
110	5.03	8.08	60	450	8.290
120	5.10	8.03	68	500	8.350
130	5.15	7.97	75	550	8.510
140	5.20	7.93			
150	5.25	7.88			
			Fuel = .889 li/min, Air = 15.034 li/min		
160	5.28	7.83	μA	V	$D_f(\text{cm})$
170	5.30	7.77	25	200	7.690
180	5.35	7.72	34	250	7.785
190	5.40	7.69	48	300	7.865
200	5.45	7.63	55	350	7.925
			60	400	8.040
			65	450	8.070
			70	500	8.085
			75	530	8.135

ROOM USE ONLY

ROOM USE ONLY



MICHIGAN STATE UNIVERSITY LIBRARIES



3 1293 03085 1103